Titre: Title:	Study on the Homogenization Speed in a Tank Equipped with Maxblend Impeller
Auteur: Author:	Maryam Hashem
Date:	2012
Type:	Mémoire ou thèse / Dissertation or Thesis
Référence: Citation:	Hashem, M. (2012). Study on the Homogenization Speed in a Tank Equipped with Maxblend Impeller [Mémoire de maîtrise, École Polytechnique de Montréal]. PolyPublie. https://publications.polymtl.ca/889/

UNIVERSITÉ DE MONTRÉAL

STUDY ON THE HOMOGENIZATION SPEED IN A TANK EQUIPPED WITH MAXBLEND IMPELLER

MARYAM HASHEM

DÉPARTMENT DE GÉNIE CHIMIQUE

ÉCOLE POLYTECHNIQUE DE MONTRÉAL

MÉMOIRE PRÉSENTÉ EN VUE DE L'OBTENTION

DU DIPLÔME DE MAÎTRISE ÈS SCIENCES APPLIQUÉES

(GÉNIE CHIMIQUE)

JUIN 2012

UNIVERSITÉ DE MONTRÉAL

ÉCOLE POLYTECHNIQUE DE MONTRÉAL

Ce mémoire intitulé:

STUDY ON THE HOMOGENIZATION SPEED IN A TANK EQUIPPED WITH MAXBLEND IMPELLER

présenté par: HASHEM Maryam

en vue de l'obtention du diplôme de : Maîtrise ès sciences appliquées

a été dûment accepté par le jury d'examen constitué de :

M. HENRY Olivier, Ph.D, président

M. FRADETTE Louis, Ph.D, membre et directeur de recherche

M. VIRGILIO Nick, Ph.D, membre

DEDICATION

To Mehdi

ACKNOWLEDGEMENTS

First of all, it is with immense gratitude that I acknowledge the support and help of my supervisor Professor Louis Fradette. I sincerely thank him for accepting me in his research group, his kind guidance, helpful suggestions, encouragement and confidence in me.

I would like to thank my committee members, Professor Nick Virgillio and Professor Olivier Henry.

Special thanks to Mr. Daniel Dumas and Mr. Jean Huard for their helps and technical support.

I would like to thank all members of URPEI group; my friends and my colleagues for their great attitude.

I would like to thank my parents, and my husband for their patience, unconditional love, and encouragements. This work was not possible without their presence.

RÉSUMÉ

Le but de ce travail est de caractériser expérimentalement la performance du mélangeur Maxblend dans le cas de suspensions solides.

De par le très grand nombre d'applications industrielles qui utilisent le mélange solide-liquide, d'importants efforts ont été mis en œuvre pour améliorer la compréhension de cette opération. Le principal objectif du mélange solide-liquide est de créer et de maintenir l'homogénéisation de la suspension. De telles opérations étant généralement réalisées dans des cuves agitées mécaniquement, le choix d'un agitateur à haute performance est primordial pour assurer à la fois la dispersion des particules et leur suspension.

L'agitateur Maxblend est un des plus efficaces parmi la nouvelle génération de mélangeur. Il est composé d'une large pale, située au bas de la cuve, et d'une grille sur la partie supérieure. La pale joue le rôle d'une pompe et la grille permet de créer la dispersion. Le mélangeur Maxblend est une alternative intéressante aux agitateurs raclant et est utilisé dans différents procédés, allant de la dispersion de gaz à la polymérisation.

Dans ce travail, une étude expérimentale a été réalisée pour caractériser la performance d'un système de mélange équipé d'un agitateur Maxblend et d'une cuve cylindrique, dans le cas des fluides newtoniens.

La vitesse d'homogénéisation (N_H), correspondant à la vitesse critique pour obtenir une suspension uniforme, est mesurée par tomographie à résistance électrique. Le travail expérimental a permis d'obtenir, pour diverses viscosités de fluides, la puissance consommée et le temps de mélange. De plus, l'impact de la géométrie de la cuve, de l'espace entre le fond de la cuve et l'agitateur, ainsi que la quantité de solide sur l'efficacité de l'agitateur à générer la suspension ont été étudiés. En se basant sur ces résultats, il est possible de confirmer que le Maxblend est un mélangeur performant, puisqu'il permet d'obtenir une suspension uniforme, un temps de mélange court avec une faible consommation d'énergie.

Mots clé: Mélange, Suspension, Solide-Liquide, Maxblend, Newtonien, fluide visqueux, Suspension homogène.

ABSTRACT

The goal of this work is to characterize experimentally the performance of a Maxblend impeller for solid suspensions.

Significant efforts have been devoted to better understand the solid liquid mixing phenomena, because of the large number of industrial applications of this operation. The major objective of solid-liquid mixing is to first create and then maintain homogenous slurry conditions. Such operations are commonly carried out in tanks stirred by suitable mechanical agitators. The important point in designing a solid-liquid suspension is choosing a high performance impeller for achieving both the dispersion of the particles and their suspension, at the same time.

The Maxblend impeller is one of the most efficient kinds of the new generation impellers. It is composed of a large bottom paddle and an upper grid. The paddle acts as a pump and the grid provides dispersion capabilities. The Maxblend impeller represents an interesting alternative to close clearance impellers and it has been used in many different processes ranging from gas dispersion to polymerizations.

In this study, an experimental investigation is carried out to characterize the mixing performance, for Newtonian fluids in a cylindrical tank equipped with a Maxblend impeller.

The homogenization speed (N_H) is introduced as the critical speed for the uniform suspension and it is measured by Electrical Resistance Tomography. The experimental work consisted in obtaining the power consumption and the mixing time for various liquid viscosities in Maxblend. Also the effects of vessel geometry, off-bottom clearance and solid loading on solid suspension efficiency are investigated. According to the results, it can be confirmed that Maxblend is an interesting technology to obtain a uniform suspension in light of short mixing time and low power consumption.

Key Words: Mixing, Suspension, Solid-Liquid, Maxblend, Newtonian, Viscous fluid, Homogeneous suspension

TABLE OF CONTENTS

LIST OF FIGURES

LIST OF TABLES

LIST OF SYBOLS

C	*Off-bottom clearance (m)*
C_D	*Drag coefficient*
C_H	*Cloud height (m)*
d_p	*Particle size (m)*
$(d_p)_{43}$	*Mass-mean particle diameter (m)*
D	*Impeller diameter (m)*
Fr	*Froude number*
g_c	*Acceleration of gravity ($m.s^{-2}$)*
H	*Liquid depth in the stirred tank (m)*
H_i	*Impeller clearance (m)*
K_p	*Power constant*
$K_p(n)$	*Power constant (for non Newtonian fluids)*
K_s	*Shear rate constant*
M	*Flow consistency index ($Pa.s^n$)*
M	*Torque (N·m)*
M_c	*Corrected torque (N·m)*
M_m	*Measured torque (N·m)*
M_r	*Residual torque (N·m)*
N	*Power-law index*
N	*Impeller rotational speed (rps)*
N_H	*Homogenization speed*
N_{js}	*Impeller speed for just-suspended (rps)*
Np	*Power number*
N^*p	*Modified power number*
P	*Power consumption (W)*
Re	*Reynolds number*
Re_p	*Particle Reynolds number*
Re_{pl}	*Power law Reynolds number*

Re_{imp}	*Impeller Reynolds number*
Re^{*}	*Modified Reynolds number*
S	*Zwietering constant*
T	*Tank diameter (m)*
T_m	*Mixing time*
V	*Voltage difference*
V_t	*Settling velocity ($m.s^{-1}$)*
V_{ts}	*Hindered velocity ($m.s^{-1}$)*
X	*Mass ratio of suspended solids to liquid (kg solid/kg liquid)*
Z	*Liquid depth in vessel (m)*

Greek Letters

P	*Density ($kg.m^{-3}$)*
ρ_l	*Liquid density ($kg.m^{-3}$)*
ρ_s	*Solid density ($kg.m^{-3}$)*
ρ^{*}	*Suspension density ($kg.m^{-3}$)*
μ	*Viscosity (Pa·s)*
μ_l	*Liquid viscosity (Pa·s)*
μ_o	*Viscosity of continuous phase (Pa·s)*
μ_r	*Relative viscosity (Pa·s)*
μ^{*}	*Suspension viscosity (Pa·s)*
N	*Kinematic viscosity of the liquid ($m^2.s^{-1}$)*
η_a	*Apparent viscosity of non Newtonian fluid (Pa·s)*
Ψ	*Sphericity*
$\emptyset$	*Volume fraction of solids in suspension (wt%)*
φ_v	*Solid volume concentration (wt%)*
$\dot{\gamma}_e$	*Effective shear rate ($1.s^{-1}$)*

Abbreviations

A100, A200, A310, A320	*Lightnin*
ERT	*Electrical resistance tomography*
CBT	*Concave Blade Turbine*
DT (n)	*Disk turbine (number of blades)*
HE-3	*High efficiency*
HF-4	*4-bladed Hydrofoil*
PBT-D (n)	*Pitched blade turbine down pumping flow (number of blades)*
PBT-U (n)	*Pitched blade turbine up pumping flow (number of blades)*
RT (n)	*Rushton turbine (number of blades)*
vol%	*Volume percent*
wt%	*Weight percent*

INTRODUCTION

Mixing processes are encountered widely throughout industry involving chemical and physical changes (Paul et al., 2004). Mixing is a central feature of many processes in the polymer processing, petrochemicals, biotechnology, pharmaceuticals, pulp and paper, coating, paints and automotive finishes, cosmetics and consumer products, food, drinking water and wastewater treatment, mineral processing, fine chemicals and agrichemicals, etc.

Despite the extensive applications of mixing, tremendous problems are very often encountered in industries due to a lack of understanding of the fundamentals involved in mixing processes.

When viewed on an international scale, the financial investment in costs of mixing processes is considerable (Nienow et al., 1997). Process objectives are crucial to the successful manufacturing of a product. If scale-up fails to produce the required product yield, quality, the costs of manufacturing may be increased significantly, and perhaps more importantly, marketing of the product may be delayed or even cancelled in view of the cost and time required to correct the mixing problem (Paul et al., 2004).

It has been estimated that 1-10 billion dollars/year are lost by North American industries due to mixing problems (Paul et al., 2004). Most industries are suffering from an oversimplified design of the mixing systems. While an oversimplified design leads to low quality products, an overly complex design is extremely costly in large scale production plants.

Although extensive experimental and numerical studies have been done on mixing systems, the successful design, operation, and scale-up of such systems still present a challenge.

Among the various mixing processes (e.g., liquid-liquid, gas-liquid, solid-liquid), solid-liquid mixing is one of the most important mixing operations, because it plays a crucial role in many unit operations, such as suspension polymerization, solid-catalytic reaction, dispersion of solids, dissolution and leaching, crystallization and precipitation, adsorption, desorption, and ion exchange (Paul et al., 2004, Zlokarnik, 2001). The major objective of solid-liquid mixing is to create and maintain homogeneity in a slurry, or to improve the rate of mass and heat transfer between the solid and liquid phases.

With this objective in mind, researchers across the world have started to study and design high performance mixing setups for solid-liquid mixing.

For low viscosity fluids the most common mixing systems are based on high speed blade turbines such as flat blade turbine, pitched blade turbine and hydrofoils in tanks equipped with baffles. In high viscosity fluids these turbines lose their efficiency because of the high clearance, dead zones and cavern effects. In order to alleviate these problems, close clearance impellers such as helical ribbon, anchor, or Paravisc rotating at low speeds could be used. These impellers provide more efficient top to bottom flow, and thus good homogenization. In solid liquid mixing of high viscosity continuous phases, usually two mechanisms are required: the first is used to reduce average particle size and the second to reach a uniform degree of dispersion throughout the vessel. A combination of the impellers mentioned above can achieve this task, resulting in the integration of several mixing step within one vessel. Multi shaft mixers can be used to carry out mixing in highly viscous systems. In many mixing processes, the rheological properties of the mixture evolve during the mixing operation. The rheology modification often originates from a chemical reaction, additives, or physical change in the solution structure. The viscosity of the final product is often higher than that of the starting material. Non-Newtonian properties may develop, depending on the nature of the reactants involved in the process. Specific types of agitators are suitable for such processes. Indeed, it is uncommon to change agitators during the reaction. Mixing specialists look for versatile agitators that can fulfill the requirements of these processes while handling the variable rheological properties.

To meet the needs of these processes with variable rheological properties a new impeller design called Maxblend has been proposed by Sumitomo Heavy Industries, Japan. It belongs to the family of the so-called “wide” impellers and has been recently introduced for the chemical process industries (See Figure 1). This impeller is mounted in a vessel with a very small clearance between the bottom wall and the lower edge of the impeller. Baffles at the vessel wall can also be installed depending on the flow regime and application in mind. The impeller’s main advantages are a precise control of the mixing flow in the vessel and the generation of a relatively uniform shear contrary to open turbines, where high shears are located in the vicinity of the turbine, yielding cavern phenomena when shear-thinning fluids are used (Solomon et al., 1981).

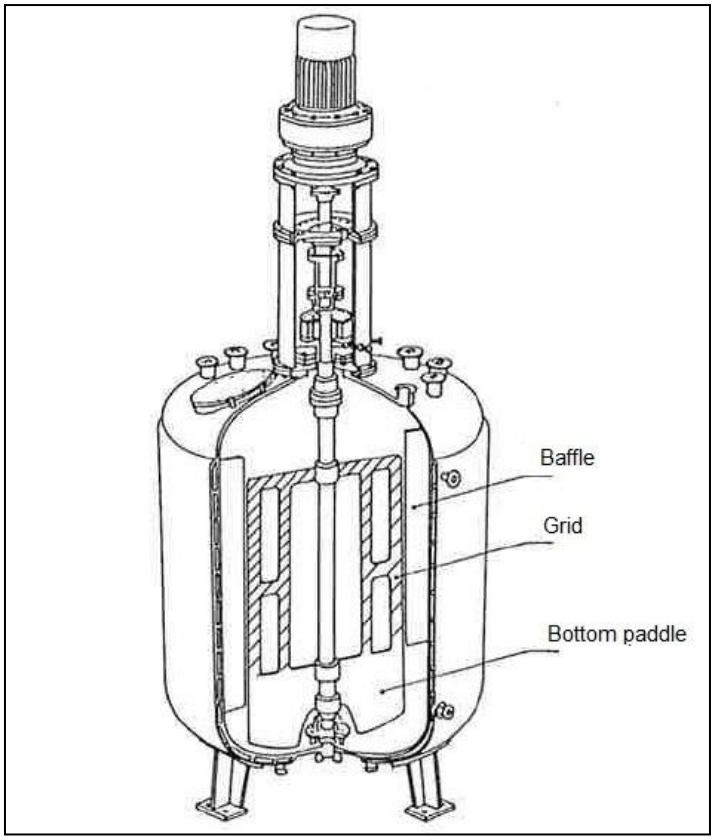

Figure 1: Maxblend reactor (SHI Mechanical & Equipment, 2001)

The mixing mechanism operated by the Maxblend is illustrated in Figure 2. The top to bottom pumping induced by the Maxblend is remarkable, the flow goes upward near the wall and downward in the center along the shaft.

This impeller is effective over a wide range of viscosities (Figure 3). It would therefore retain a high mixing efficiency for many processes, regardless of viscosity changes during mixing.

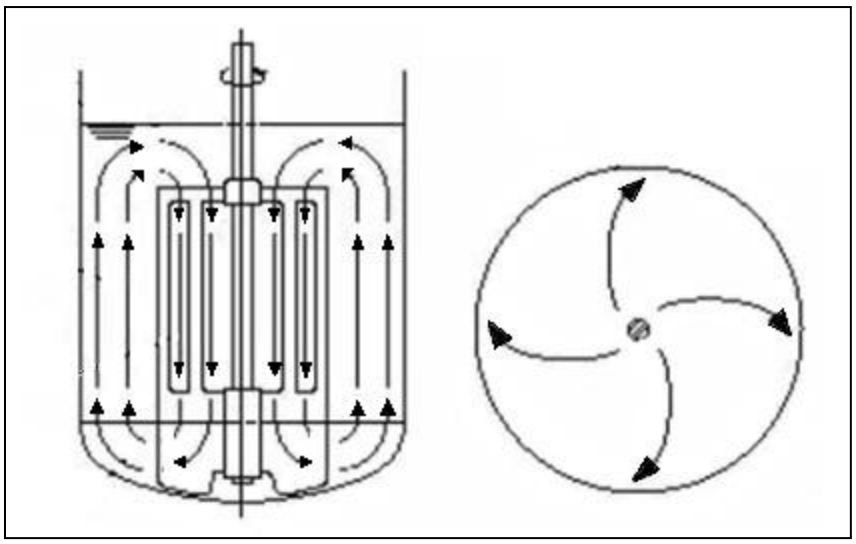

Figure 2: Mixing mechanism (SHI Mechanical & Equipment, 2001)

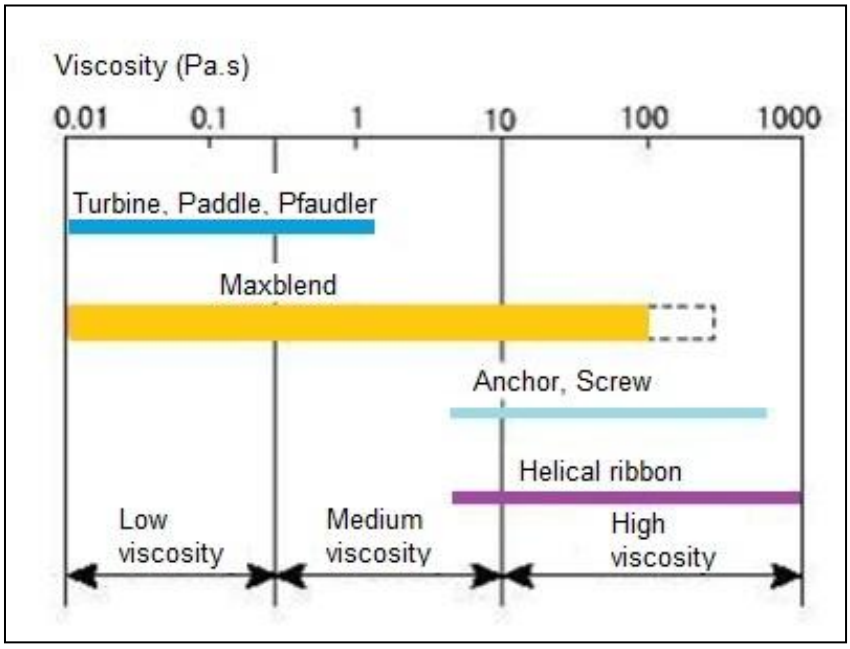

Figure 3: Range of Maxblend impeller efficiency (SHI Mechanical & Equipment, 2001)

SHI uses the Maxblend for a variety of applications in liquid-liquid, liquid-solid and gas-liquid mixing. According to the manufacturer claims, the Maxblend can handle processes from suspension polymerization and crystallization operation to high viscosity gas absorption (Table 1).

Table 1: Applications of Maxblend mixer

Mixing Medium	Process/Operation	Product/Application Example
Solid -Liquid Mixing	Suspension Polymerization Crystallization Operation Salting-Out, Oxygenation-Out Powder and Resin Dissolution	PVC, PS, Water Adsorbent Polymer Cooling, Reaction, Condensation Clam Former, ABS Precipitation PVA, CMC, Lignin
Liquid-Liquid Mixing	Emulsion Polymerization Solution Polymerization Bulk Polymerization Condensation Polymerization	ABS, Paste PVC, Vinyl Acetate, Acrylic Emulsion AS, BR, Thermoplasticity Elastomer PS, PMMA, Spandex Biodegradable Polymer
Gas-Liquid Mixing	Hydrogenation, Chlorination EO, PO Addition Reaction High Viscosity Gas Absorption High Viscosity Cultivation	Polymer Hydrogenation, Oils and Fats, Amine Surfactant Thermoplastic Elastomer etc. Biopolymer, Bio-Cellulose

Although these claims make this impeller pretty attractive for solid-liquid mixing applications, in practice, the actual performance of the impeller is not well documented. The objective of this work is to describe the solid-liquid mixing behavior when using a Maxblend. The project considers Newtonian viscous mixing. We are especially interested in the performance characteristics of this impeller and how they compare when the impeller operates in different operating and design conditions. The study is performed experimentally.

CHAPTER 1

LITERATURE REVIEW

1.1. Solid Suspension

Dispersion generally consists of discrete particles randomly distributed in a fluid medium. Dispersion can be divided into three categories: solid particles in a liquid medium (suspension), liquid droplets in a liquid medium (emulsion) or gas bubbles in a liquid (foam). Suspension is the dispersion of particulate solids in a continuous liquid phase, which is sufficiently fluid to easily circulate by a mixing device (Uhl and Gray, 1986). However, in the case that a system incorporates powders and fine particles throughout the liquid medium is considered as dispersion or colloidal suspension (Harnby et al., 1997). When the particle concentration and, for a range of sizes, the size distribution is constant throughout the tank, homogeneous suspension exists (Harnby et al., 1997). The quality of solid suspension can be divided into three regimes: on-bottom (partial), off–bottom (complete) and homogeneous (uniform) suspension regimes (Paul et al., 2004). These are illustrated in Figure 1-1.

On-bottom motion or partial suspension: This situation can be described as the complete motion of all solid particles in the whole tank, regardless of aggregation of particles in corners or other parts of the tank bottom, which means there are still some particles in motion that have contact with the tank bottom. In this case, not all the surface area of particles is available for chemical reaction or mass or heat transfer. This condition is sufficient for the dissolution of solids with high solubility.

Off-bottom or complete suspension: This situation can be described as the complete motion of particles where no particle lays on the tank bottom for more than 1 to 2 seconds, even though the suspension throughout the tank might not be uniform. Due to this whole motion, the surface area reaches the maximum level for the chemical reaction and diversity of transfer. Since this situation

is the minimum mixing requirement in most solid-liquid systems, the "just suspended speed" is always chosen as an important parameter in the study of the solid-liquid system.

Uniform suspension: This situation can be described as the formation of both uniform particle concentration and particle size distribution in the whole tank. Any further increase in impeller speed or power does not appreciably improve the solids distribution. This condition is required for crystallization and solid catalyzed reaction.

Suspension percentage,

$$\frac{\text{The weight percentage of the solids in sampling spot}}{\text{The average weight pencentage of the solids in the whole tank}} \times 100\% , \quad (1\text{-}1)$$

might be greater than, equal to, or smaller than 100%. As for the uniform suspension, the suspension percentage is 100%. Basically, by increasing the power input or rotating speed, the particle distribution does not obviously improve. This suspension is required in processes, such as the crystallization process and solid catalyzed reaction, where uniform solids concentration is vital to the efficiency of an operation unit or even the continuity of a whole production line. Of course, this ideal scenario is based on more power input, more effective equipment configuration, and certain operating conditions.

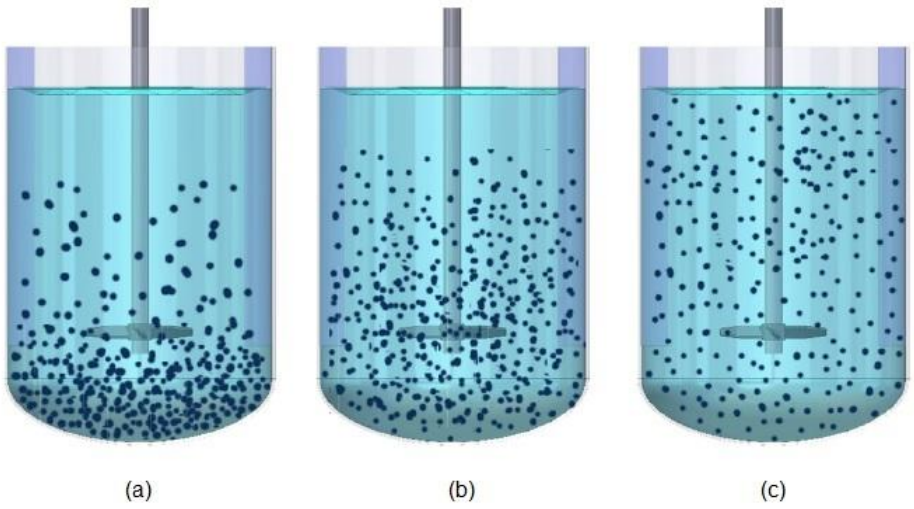

Figure 1-1: Degrees of suspension. (a) Partial suspension, (b) Complete suspension, (c) Uniform suspension (Tahvildarian et al., 2011)

Distribution and dispersion are discussed when the quality of solid-liquid mixing is studied. The uniform suspension depends on both good distribution and dispersion. Figure 1-2 presents examples to clarify the difference between distribution and dispersion. In the first row, aggregations exist in both conditions. In Figure (a), the particles aggregate randomly resulting in a bad distribution and a bad dispersion. In (b), aggregations distribute orderly which is considered as a good distribution and a bad dispersion. Figure (c) demonstrates a good dispersion and a bad distribution where there are still some aggregations from a microscopic perspective, but for each aggregation, the distribution of particles is uniform. Finally in (d), there is no aggregation and particles distribute uniformly within the tank in what is called uniform suspension.

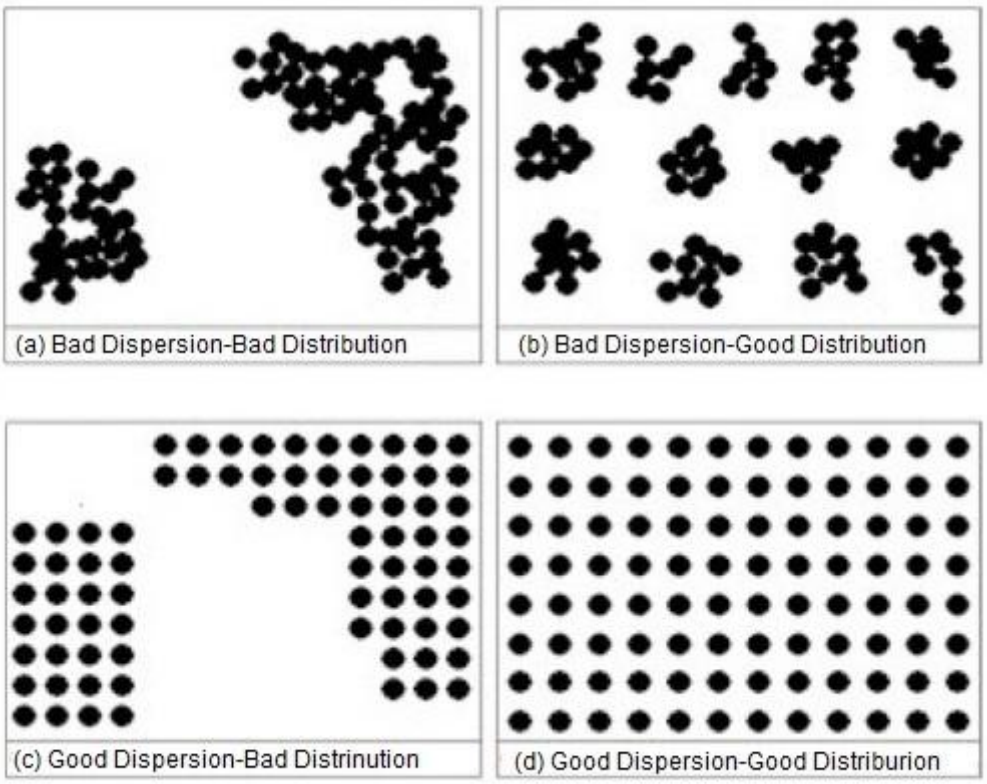

Figure 1-2: Distributive mixing versus dispersive mixing

The physical and chemical properties of liquid and solid particles influence the fluid-particle hydrodynamics and, consequently, the suspension. For example, large, dense solids are more difficult to suspend than small particles with low density in the same continued phase. Another

example is spherical particles, which are more difficult to suspend than thin flat disks (Paul et al., 2004). The properties of both the solid particles and the suspending fluids influence the suspension. Also vessel geometry and agitation parameters are important. The important liquid and solid properties and operational parameters are as follows:

a) Physical properties of the continuous phase:
   - Liquid density, ρ_l
   - Density differences, ρ_s-ρ_l
   - Liquid viscosity, μ_l

b) Physical properties of solid particles:
   - Solid density, ρ_s
   - Particle size, d_p
   - Particle shape or sphericity
   - Wetting characteristics of the solid
   - Tendency to entrap air or head space gas
   - Agglomerating tendencies of the solid
   - Hardness and friability characteristics of the solid

c) Process operating conditions:
   - Liquid depth in vessel
   - Solids concentration

d) Geometric parameters:
   - Vessel diameter
   - Bottom head geometry: flat, dished, or cone-shaped
   - Impeller type and geometry
   - Impeller diameter
   - Impeller clearance from the bottom of the vessel
   - Baffle type, geometry, and number of baffles

e) Agitation conditions:
   - Impeller speed, N
   - Impeller power, P

For example, for small solid particles, which have a density approximately equal to the liquid, once suspended they continue to move with the liquid. The suspension behaves like a single-phase liquid at low solid concentrations. For solid particles with higher density their velocities are different from that of the liquid. The drag force on the solid particles caused by the liquid motion must be sufficient and directed upward to counteract the tendency of the particles to settle by the gravity force.

Solid suspension processes consume a huge amount of processing time and energy, so it is necessary to know about the various factors affecting them. There are some studies investigating these parameters such as the following:

a) Physical properties of liquid, such as density and viscosity (Chapman et al., 1983, Ibrahim and Nienow, 1994).

b) Physical properties of solid, such as density, particle size, sphericity, wetting characteristics of solid, agglomerating tendencies of the solid and hardness and friability characteristics of the solid (Altway et al., 2001, Ayranci and Kresta, 2011).

c) Process operating conditions, such as liquid depth in the vessel and solid concentration (Einenkel, 1980).

d) Geometric parameters, such as vessel diameter, bottom head geometry like flat, dished or cone-shaped, impeller type and geometry, impeller diameter, impeller clearance from the bottom of the vessel, baffle type and the geometry and number of baffles (Biswas et al., 1999, Wu et al., 2001).

e) Agitation conditions, such as impeller speed, impeller power, impeller tip speed, level of suspension achieved and liquid flow pattern (Biswas et al., 1999).

1.1.1. Settling Velocity

When a dense solid particle is placed in a motionless fluid, it will accelerate to a steady-state settling velocity, which is called the free settling velocity. It occurs when the drag forces balance the buoyant and gravitational forces of the fluid on the particle. However, in equilibrium the sum of these forces is zero.

In Newtonian fluids for spherical particles, the free settling velocity (v_t) is a function of different physical and geometrical parameters and it is defined by

$$V_t = \left[\frac{4g_c d_p(\rho_s - \rho_l)}{3C_D\rho_l}\right]^{1/2}. \quad (1\text{-}2)$$

In this equation, C_D is the drag coefficient, which directly depends on the particle Reynolds number (Re_p),

$$Re_p = \frac{\rho_l V_t\, d_p}{\mu}, \quad (1\text{-}3)$$

and particle shape. The expression of the drag coefficient for each flow regime is defined in Table 1-1. By substituting each definition of drag coefficient in equation 1-2, the terminal velocity for each regime, in the case of low concentration suspensions, could be calculated (Paul et al., 2004).

Table 1-1: Hydrodynamic regimes for settling particles (Paul et al., 2004)

Regime	Re_p	C_D
Stokes' law(laminar)	$Re_p < 0.3$	$C_D = 24/ Re_p$
Intermediate law	$0.3 < Re_p < 1000$	$C_D = 18.5/ Re_p^{3/5}$
Newton`s low (turbulent)	$1000 < Re_p < 35\times10^4$	$C_D = 0.445$

1.1.2. Hindered Settling

In the case of low concentration suspensions, the settling velocity can be evaluated using equation 1-2. However, when the concentration is increased (>2%) particle-particle interactions become significant and other particles decrease the value of V_t (Blanc and Guyon, 1991). Hindered velocity occurs because of interactions with surrounding particles, interaction with the

upward flow of fluid created by the downward settling of particles, or increase in the apparent suspension viscosity and density. An empirical correlation for hindered settling velocity is reported by Maude as

$$V_{ts} = V_t(1 - \emptyset)^n, \tag{1-4}$$

where V_{ts} is the hindered settling velocity, V_t is the settling velocity, $Ø$ is the volume fraction of solids in suspension, and n is a function of the particle Reynolds number (Re_p) which is defined as follows (Maude and Whitmore, 1958):

Table 1-2: Values of the exponent in Maude empirical correlation

$Re_p < 0.3$	n = 4.65
$0.3 < Re_p < 1000$	$n = 4.375\ Re_p^{-0.0875}$
$1000 < Re_p$	n = 2.33

This expression is recommended for preliminary estimates of the effect of solid concentration on settling velocity (Paul et al., 2004).

1.1.3. Rheological Properties of Suspension

Rheology is the science of flow and deformation of materials. The rheology of suspensions is an important subject in the field of rheology since it shows various types of rheological characteristics, such as thixotropy, shear thinning, shear thicking, viscoelastic, etc. We need to develop our knowledge about suspension rheology for a wide range of industrial applications, such as paint, ink, cement, cosmetics, food, and agricultural products in order to select the best production conditions for the specific application.

The viscosity of slurry is a function of the continuous phase viscosity, particle-particle interactions, and the size distribution, concentration, and the shape of particles. It is also a

function of the shear rate, and can be a function of the shearing time (Shamlou, 1993). Suspensions are classified depending on the rheological behaviour of the continuous phase (Jinescu, 1974).

a) Suspension in a Continuous Newtonian Phase
b) Suspension in a Continuous Non-Newtonian Phase

In Newtonian continuous phase, Newtonian behavior is observed for small solid concentrations, whereas the suspension is usually non-Newtonian for high solid concentration (Shamlou, 1993).

For non Newtonian medium, a suspension shows non-Newtonian behaviour even with small concentrations of solid particles. In small solid particle concentrations, the non-Newtonian behaviour is caused by the continuous phase. However, with high concentrations of solid particles, particle-particle interactions usually heighten the non-Newtonian behaviour of the suspensions.

For non-Newtonian shear thinning liquids, higher agitator speeds can be expected than for Newtonian liquids, especially where a single impeller is used. This is due to the rapid fall-off in fluid motion away from the impeller. Hence for very shear thinning fluids a multi impeller is recommended; also large diameter impellers are more effective at creating movement at the liquid surface than small impellers and so are more effective at drawing solids into the liquid (Shamlou, 1993).

Many experimental and theoretical works have been carried out to predict the rheological behaviour of suspensions. These models were derived under the assumption of spherical, rigid and mono-dispersed particles.

For example, for the viscosity of suspension, which contains a volume concentration of spherical solid particles up to 50%, Gillies et al. derived an equation, which is in good agreement with experimental results (Gillies et al., 1999):

$$\mu_r = \mu\left[1 + 2.5\varphi + 10.05\varphi^2 + 0.00273\exp(16.6\varphi)\right], \tag{1-5}$$

where μ_r is relative viscosity, φ is the volume fraction of the spheres. In this equation the terms of an order of two and higher are a result of particle-particle interactions in highly concentrated suspensions.

1.2. Solid-Liquid Suspension in Mechanically Agitated Vessels

1.2.1. Hydrodynamic Regimes

Suspension of solid particles needs the input of mechanical energy into the solid-liquid system by some mode of agitation. The input energy makes a turbulent flow field in which solid particles are lifted from the base of vessel and then dispersed and distributed throughout the liquid.
Nienow discussed in some detail the complex hydrodynamic interactions between solid particles and fluids in mechanically agitated tanks. First, there is a drag force on particles arising from the boundary layer flow across the bottom of the tank. To suspend the particle the velocity of the boundary layer flow should be ten times greater than the particle settling velocity in a motionless fluid. Second, turbulence breaks the boundary layer and if the frequency and energy levels are high enough, a suspension will be started (Nienow et al., 1997). Latest measurements of the 3D velocity of both the solid particles and the fluid confirm this complexity (Paul et al., 2004). Solids pickup from the tank bottom is achieved by a combination of the drag and lift forces of the moving fluid on the solid particles and the bursts of turbulent eddies originating from the bulk flow in the tank. Among the various models which explain the hydrodynamics of solid-liquid suspensions, the most successful one was proposed by Baldi et al.. According to his model, the particles in the vessel base are suspended mainly due to turbulent eddies of approximately the same scale as the particle size (Baldi et al., 1978).

1.2.2. Solid-liquid Dispersion in High Viscous Continuous Phase

When the continuous phase viscosity is considered to be low enough to reach a turbulent regime, obtaining a uniform suspension is a difficult task due to the high settling velocity of the particles. In most industries dealing with food, polymer, pharmaceutical and biotechnological processing, mixing involves high viscosity medium or low rotating speeds, which means operating at the laminar regime.

Processing these high viscosity materials may require the incorporation of fine solids. To achieve a solid dispersion in a viscous continuous phase, the objective is to produce a uniform material with an acceptably low level of agglomerates of the basic individual particles.

In high viscosity continuous phases, in the absence of turbulent eddies, the stresses, which are produced within the liquid during laminar flow, are responsible for breaking and rupturing agglomerates of particles and dispersing them uniformly as individual particles throughout the vessel. In the absence of molecular diffusion, this mechanism tends to reduce the size and scale of the unmixed clumps. High shear stresses for such a task can be achieved in mixers which provide high shear and the components should pass through these zones as often as possible. In mixers handling high viscosity fluids (such as Rneaders, internal mixers, planetary mixers, and helical ribbons) the flow patterns are very complex. All of these mixers incorporate high shear zones and regions where fluids are redistributed. The shear produced, however, in the high shear zones of these mixers may not be enough to reduce the size of the agglomerates and break the lumps as required. In this case, incorporation of a high shear mixer and a distributive mixer for high viscosity continuous phases would improve the mixture quality.

1.2.3. Just Suspension Speed in Stirred Tanks (N_{js})

The minimum impeller speed at which all the particles reach complete suspension is known as N_{js}. Under this condition, the maximum surface area of the particles is exposed to the fluid for chemical reaction or mass or heat transfer. The “just suspended” situation refers to the minimum agitation conditions at which all particles reach complete suspension.

Many efforts have been made to characterize this parameter experimentally, and theoretically which result in different equations for predicting it.

One of the first studies in this field was done by Zwietering (Zwietering, 1958). He introduced the visual observation method to find out N_{js}. The motion of the solid particles on the tank bottom was visually observed through the transparent tank. N_{js} was measured as the speed at which no solids are visually observed to remain at rest on the tank bottom for more than 1 or 2 seconds.

Simplicity is the main advantage of visual methods. However, only with careful and experienced observation it is possible to achieve ±5% reproducibility in a diluted suspension. Furthermore,

visual methods need a transparent vessel, which is feasible for most laboratory-scale studies, but rather out of reach for large-scale tanks. To overcome the limitations of the visual method other techniques have been proposed and different concepts have been applied, like solid concentration change directly above the vessel bottom (Bourne and Sharma, 1974a, Musil and Vlk, 1978), ultrasonic beam reflection from the static layer of the solid on the vessel base (Buurman et al., 1986), variation of power consumption or mixing time (Rewatkar et al., 1991), pressure change at the bottom of the vessel (Micale et al., 2000, Micale et al., 2002).

Experimental techniques have been used to perform many empirical and semi-empirical investigations on solid suspension, results of which have been critically reviewed in the literature (Armenante and Nagamine, 1998, Armenante et al., 1998, Paul et al., 2004, Harnby et al., 1997). Most presented correlations have been developed based on the visual technique. Most of the studies resulted in modifications of model parameters in the Zwietering correlation. Zwietering derived the following correlation from dimensional analysis. He estimated the exponent by fitting the data to the just-suspended impeller speed (Zwietering, 1958),

$$Njs = Sv^{0.1}\left[\frac{g_c(\rho_s - \rho_l)}{\rho_l}\right] X^{0.13}\, d_p\, D^{-0.085}\,, \tag{1-6}$$

where:

$$S = Re_{imp}^{0.1}\, Fr^{0.45}\left(\frac{D}{dP}\right)^{0.2}\, X^{0.13}\,, \tag{1-7}$$

$$Re_{imp} = \frac{N_{js}D^2}{v}, \tag{1-8}$$

$$Fr = \frac{\rho_l N_{js}^2\, D}{(\rho_s - \rho_l)g_c}, \tag{1-9}$$

where D is the impeller diameter, d_p is the mass-mean particle diameter $(d_p)_{43}$, X is the mass ratio of suspended solids to liquid × 100, S is the dimensionless number which is a function of impeller type, v is the kinematic viscosity of the liquid, g_c is the gravitational acceleration constant, and ρ_s and ρ_l are the density of particle and the density of liquid, respectively.

He showed that in the calculation of N_{js} a significant variance appears and there is no correlation with universal validity. Bohnet (Bohnet, 1980) determined N_{js} using nine correlations to find that

the reported values were in the range of -56% to +250% from their own value. Different empirical correlations have been developed based on experimental characterization of N_{js}. Prediction of N_{js} was a subject of few CFD studies (Fletcher and Brown, 2009, Lea, 2009, Murthy et al., 2007, Panneerselvam et al., 2008). Kee and Tan presented CFD approach for predicting N_{js} and characterized effect of D/T and C/T on N_{js} (Kee and Tan, 2002).

1.2.4. Cloud Height

In solid suspension, there is a distinct level at which most of the solids become lifted within the fluid. This height of the interface from the bottom of vessel is called cloud height and above this interface there are only a few solid particles. Liquid below this height, however, is solid-rich (Bittorf and Kresta, 2003). Measurement of cloud height within the stirred vessel provides a qualitative indication of suspension quality. Many studies have been done to express homogeneity as a function of cloud height (Bujalski et al., 1999, Hicks et al., 1997, Ochieng and Lewis, 2006b, Oshinowo, 2002). Cloud height is considered as a global parameter and cannot provide satisfactory information on local mixing quality.

Bittorf and Kresta derived an equation for cloud height that corroborates the best results for solids distribution at low clearance and for a large impeller diameter (Bittorf and Kresta, 2003):

$$C_H = \frac{N}{N_{js}}\left(0.84 - 1.05\left(\frac{C}{T}\right) + 0.7\frac{\left(\frac{D}{T}\right)^2}{1-\left(\frac{D}{T}\right)^2}\right), \tag{1-10}$$

where C_H, N, N_{js}, C, D and T are cloud height, impeller speed, just suspended impeller speed, clearance, impeller diameter, and tank diameter, respectively.

1.2.5. Mixing Time

Mixing time is a parameter commonly used to characterize the mixing performance of impellers in agitated vessels. It is defined as the time required to reach a certain degree of local homogeneity. Quantitative mixing time measurements, which can be carried out using several different methods, give us a qualitative understanding of mixing behavior. The most appropriate technique for mixing time measurement depends on the fluid specifications and the mixing scenarios. Many physical and chemical methods have been developed with various degrees of success. However, since each technique has its own limitations, there is no universally accepted technique for mixing time measurement. The mixing time measurement methods can be divided into two groups based on the volume of fluid involved in the measurement; local and global techniques. The local measurement methods rely on physical measurements made with intrusive probes. They provide a single mixing time, which is the time necessary to reach a given degree of homogeneity at a given location. However, more than one probe can be applied in a vessel to partially circumvent the problem of local measurement. Thermal methods, conductometric methods, fluorimetric methods, and pH based methods are examples of this measurement technique. The global measurement methods are either chemical-based, involving a fast reaction (e.g., acid-base and redox color change methods) or optical-based likes Schlieren's method. The global methods possess instructive features such as the capability to identify—and very often quantify—the unmixed zones. Also, the global methods can measure the mixing end point. They are nonintrusive and they do not perturb the flow. However, they are usable only in transparent laboratory vessels. One main drawback of these techniques is the subjectivity of the measurement interpretation. Indeed, the mixing time is typically determined with the naked eye and may yield different results if the same experiment is realized by different individuals or repeated many times by the same operator.

1.2.6. Power Consumption

In fact one important parameter in the design and operation of mechanically agitated vessels is the amount of power dissipated in the vessel by the impeller. For designing a process system, the selection of the most appropriate mixing system according to the process specifications is a significant task. The selection criterion is often based on mixture quality (homogenization) and power consumption (Holland and Chapman, 1966).

Generally in Newtonian fluids, the power consumption of an impeller is expressed in terms of power number,

$$Np = \frac{P}{\rho\, N^3 D^5}\,. \tag{1-11}$$

For constant geometrical relationships and negligible gravitational influence, the power number depends only on the impeller Reynolds number,

$$Re = \frac{\rho N D^2}{\mu}. \tag{1-12}$$

In a laminar regime the power number is inversely proportional to the Reynolds number,

$$N_P = \frac{K_P}{Re}, \tag{1-13}$$

where K_p is a constant, that depends on the geometry of the mixing system. In a transitional regime there is no simple expression for N_p vs. *Re*.

For non-Newtonian fluids where the apparent viscosity of the fluid varies as the shear rate changes, predicting the power consumption is complicated. A means of dealing with this difficulty was first proposed by Metzner and Otto for a non-Newtonian fluid in a laminar regime based on calculations of apparent viscosity for mixers. The basic assumption of this method is that there is an effective shear rate for a mixer, which can describe the power consumption and this shear rate is proportional to impeller speed (Metzner and Otto, 1957),

$$\dot{\gamma}_e = K_s N\,, \tag{1-14}$$

where K_s is a shear rate constant, which depends on the geometry of the impeller and $\dot{\gamma}_e$ is an effective shear rate, which defines an apparent viscosity for predicting power consumption in non-Newtonian fluids. In order to determine the value of K_s, the following steps are proposed:

- For a specific rotational speed (N), the power consumption can be determined experimentally, and the power number for non-Newtonian fluids can be calculated from equation (1-10).
- From the Newtonian power curve, find the Reynolds number corresponding to the non-Newtonian power number. This Reynolds number is known as the generalized Reynolds number (Re_g). The apparent viscosity is calculated from the following equation:

$$Re_g = \frac{\rho N D^2}{\eta_a}. \tag{1-15}$$

- From the curve of viscosity versus shear rate, which can be obtained experimentally, the shear rate can be found according to the apparent viscosity.
- Finally, the slope of effective shear rate versus rotational speed gives the value of K_s.

The value of K_s, can also be determined by mathematical manipulation. By substituting Newtonian viscosity (μ) by the apparent viscosity of the non-Newtonian fluid (η_a) in the expression for K_p (due to the fact that our non-Newtonian fluids obey the power law):

$$\eta = m|\dot{\gamma}|^{n-1}. \tag{1-16}$$

We obtain:

$$N_p = \frac{K_p}{Re} = \frac{K_p m (K_s N)^{n-1}}{\rho N D^2} = \frac{K_p {K_s}^{n-1}}{Re_{pl}}. \tag{1-17}$$

Based on the fact that $K_p\,(n) = N_p \,.\, Re_{pl}$,

$$K_s = \left(\frac{K_p(n)}{K_n}\right)^{\frac{1}{n-1}}. \tag{1-18}$$

This method can also be generalized for Bingham fluids and Hershel-Bulkley fluids. From these correlations, two power measurements, one for Newtonian fluids and one for non-Newtonian fluids of known viscosities, are enough to obtain K_s.

For power consumption in suspensions few investigations have been done. Pasquali et al. were the first to estimate the power curve for suspensions of rigid, spherical particles of uniform size with maximum 30% volume of solid concentration in Newtonian fluids. Afterwards, for solid - liquid suspensions, they introduced the modified power number and modified Reynolds number as

$$N_P^* = \frac{P}{\rho^* N^3 D^5} \tag{1-19}$$

and

$$Re^* = \frac{\rho^* N D^2}{\mu^*}, \tag{1-20}$$

where ρ^* is density and μ^* is the viscosity of the suspension (Pasquali et al., 1983). These two parameters are defined as

$$\rho^* = \emptyset_v \, \rho_s + (1 - \emptyset_v)\rho_l \tag{1-21}$$

and

$$\mu^* = \mu_l(1 + 2.5\emptyset_v + 10.05\emptyset_v^2 + 0.00273 \exp(16.6 \, \emptyset_v)), \tag{1-22}$$

where $\emptyset_v$ is the solid volume concentration. In this manner, they observed that the modified power curve (N_p* vs *Re**) superimposes the single phase power curve (N_P vs *Re*). Consequently, the power consumption of solid-liquid mixing can be estimated if the single phase power curve is known, as well as the density of the suspension (defined as the total mass in the vessel divided by the total volume) and the volume fraction of particles (Figure 1-3).

Bujalski (Bujalski et al., 1999) determined the power number for the A-310 impeller (hydrofoil) for solid loading up to 40 wt% . They showed that by increasing the solid loading, the power number increases. At solid loading higher than 20 wt% the variation of power number showed different trends. At low impeller speeds (N<200 rpm) the power number is lower than that for the single phase. By increasing impeller speed the power number increases until it reaches a maximum value and then it slightly decreased. The constant value of the power number at higher impeller speeds was higher than that for the single phase and it is related to solid concentration, which affects the mixture density surrounding the impeller.

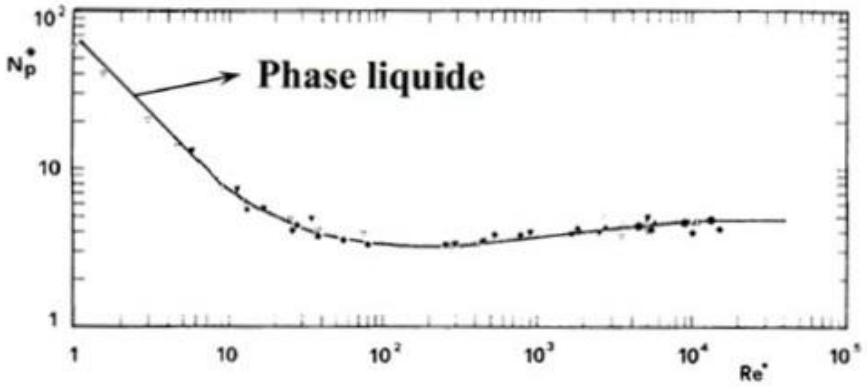

Figure 1-3: Power curve for solid suspension in compare with single phase (Pasquali et al., 1983)

Bujalski et al. related the lower power variation to bottom shape change by increasing impeller speed. They have mentioned that at low speed the presence of a solid layer at the bottom of the vessel redirected the flow and the overall effect is that the power number is reduced. By increasing impeller speed this layer starts to vanish and the power number increases.

Wu et al. investigated power number variation for PBT-D and RT at extreme solid concentrations (>50 vol %). They found, the power number of PBT increases at high solid concentrations while that of RT decreases (Wu et al., 2002). Increasing the power number for PBT can be explained in the same way as Bujalski et al. (Bujalski et al., 1999) did, but a reduction in the power number of RT was related to the fact that damping at high solid loading suppresses the dead flow zones at the back of the Rushton turbine blades leading to the reduction of drag. On the other hand there is no dead flow zone behind the Rushton turbine blades and increasing solid loading only increases skin friction and, accordingly, drag coefficient. Those results are in contrast with what has been reported by Angst and Karume (Angst and Kraume, 2006), who reported the reduction of the power number for the Pitched blade turbine.

1.3. Impeller for Solid-liquid Suspension

The impeller plays several tasks in the agitation vessel; to suspend solid particles and to disperse them effectively. Choosing the proper impeller to satisfy the required solid suspension with a minimum power requirement is the key for the technical and economic viability of the process. There are two regions at the tank bottom where recirculation loops are weak: underneath the impeller and at the junction of the tank base and wall. N_{js} is affected significantly by the region of the vessel where the final portions of the settled solid particles are lifted into suspension. This region varies for different impeller types. Impellers are classified as radial or axial flow impellers. Flow pattern of axial and radial flow impellers are completely different. Differences in flow pattern leads to different solid suspension mechanisms. Radial flow impellers sweep particles toward the center of the vessel base and suspend them from an annulus around the center of the vessel bottom. On the other hand, axial flow impellers tend to suspend solid particles from the periphery of the vessel bottom. It is more difficult to lift particles from the center than drive them toward the corner. The flow pattern of axial flow impellers facilitates suspension in comparison to radial flow impellers.

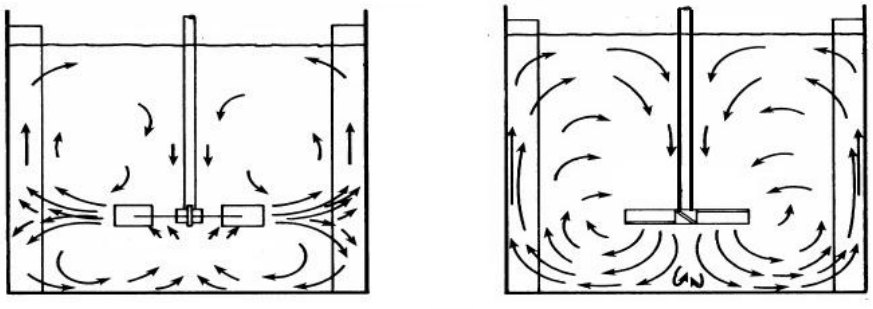

Figure 1-4: Radial and axial flow pattern

For impeller selection it is important to identify which impeller can provide the required hydrodynamics for the process at lower power consumption. In addition it is necessary to have information on cloud height, solid concentration distribution, and mixing-reaction contributions to make the proper selection.

In a turbulent liquid, suspending solid particles can be considered as balancing energy supplied by a rotating impeller and energy needed to lift the solids. Axial flow impellers with high pumping efficiencies are most appropriate for solids suspension. These impellers generate a flow pattern which sweeps the bottom of tank and suspends the particles. Solid pickup from the vessel base is achieved by a combination of the drag and lift force of the moving fluid on the solid particle and the bursts of turbulent eddies originating from the bulk flow in the vessel (Paul et al., 2004).

In solid-liquid mixing with high viscosity continuous phases, usually two mechanisms are required: the first is used to reduce particle size distribution and the second to reach a uniform degree of dispersion homogeneity throughout the vessel. A combination of the impellers mentioned above can achieve this task, resulting in the integration of several mixing steps within one vessel. In practice, the following mixing systems are found in industry (Tanguy et al., 1997):

- Multiple intermeshing kneading paddles mounted on a carousel (planetary mixer).
- A main centered impeller associated with off-centered ancillary turbines located close to the vessel surface.
- Co-axial impellers of a similar type rotating at the same speed.
- Co-axial or contra-rotating coaxial impellers with different speeds.

The existence of a scientific basis behind the development of these types of mixing systems is rare, as they have been developed by empirical considerations and industrial experiences. Many studies were done to find more effective impellers for solid-liquid suspensions. These investigations have shown that axial impellers have better performances (Paul et al., 2004).

Lightnin impellers, such as A100, A200, A310 and A320, are used in different studies. These impellers make high downward flow pumping. Using ligtnin impellers in a flow controlled operation, e.g. solid suspension, is more cost effective than other axial impellers (McDonough, 1992).

Cooke and Heggs reported that the hollow blade turbine is an efficient impeller for the solid-liquid mixing operations under gassed conditions (Cooke and Heggs, 2005). Bararpour investigated the dual shaft mixer consisting of a wall-scraping Paravisc and a high speed Deflo disperser (Bararpour et al., 2007). Lea employed a Standard 45˚ pitch 6-bladed turbine (Lea,

2009) and Sardeshpande et al. used a down-pumping, pitched 6-bladed turbine (PBTD-6) and a 4-bladed Hydrofoil (HF-4) in their work (Sardeshpande et al., 2009).

Lehn et al. compared power consumption for different impellers (Figure 1-5). Knowledge on power consumption in solid-liquid stirred tank is essential for proper design and operation (Lehn et al., 1999).

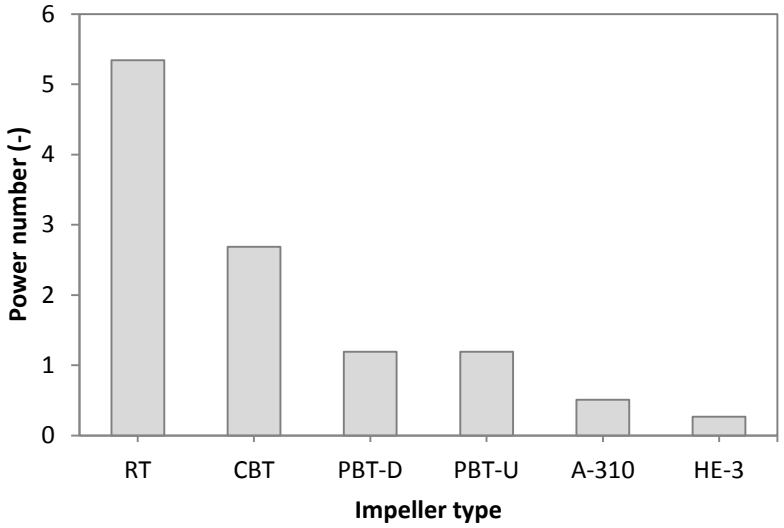

Figure 1-5: Ungassed power number of impellers in turbulent regime for different impellers (Lehn et al., 1999)

Some researchers have studied solid-liquid mixing in agitated vessels through experimental investigation (Baldi et al., 1978, Bujalski et al., 1999, Hicks et al., 1997, Wu et al., 2001) and some have employed CFD to explore the effect of impeller type on C_H and N_{js} (Oshinowo, 2002, Micale et al., 2004). Sardeshpande et al. investigated the effect of solid volume fraction and impeller speeds on the N_{js}, C_H, power consumption, mixing time, and circulation time using PBTD and HF impeller. They used tap water and glass bead particles (50-250 μm) with 1, 3, 5, and 7 vol% loading. They developed a new way of characterizing solid-liquid suspensions and liquid phase mixing using nonintrusive wall pressure fluctuation measurements. They found out that at higher solid loading (above 3 vol%), cloud height measurements indicated different stages of suspension. By increasing impeller speed under certain conditions, cloud height is decreased. Interaction of incompletely suspended solids, a bed of unsuspended solids at the bottom and impeller pumping action cause such non-monotonic variations of cloud height with the impeller

speed (Sardeshpande et al., 2009). Giraud et al. showed that the optimal impeller speed has a significant effect on the degree of homogeneity. This speed should always be between two critical impeller speeds, N_{js} and the impeller speed for the maximum homogeneity, preferably closer to the latter. Also, by increasing the particle size, the free settling velocity in solid suspension is increased and the extent of homogeneity is decreased (Guiraud et al., 1997).

Most of the studies on just suspended speed have been carried out in flat bottom vessels. A few work attempted to characterize N_{js} in dish bottom vessels (Buurman et al., 1986) or studied the effect of tank bottom shape (Chudacek, 1985, Musil and Vlk, 1978). Ghionzoli et al. studied the effect of bottom roughness on N_{js}. They have reported that effect of bottom roughness is related to particle size. For small particles size, suspension is helped by roughness. But by increasing d_p rough bottom begin to hinder suspension (Ghionzoli et al., 2007). The influence of the clearance on the flow pattern has been the subject of extensive studies. (Kresta and Wood, 1993, Bourne and Sharma, 1974b, Sharma and Shaikh, 2003). Montante et al. investigated transition in flow pattern for RT by decreasing impeller clearance by means of laser-Doppler anemometry (Micale et al., 2000, Montante et al., 1999). they also studied flow regime transition for RT by means of CFD tools For axial flow impellers (Montante et al., 2001, Micale et al., 2004, Micale et al., 2000). Sharma and Shaikh showed that all impellers with very low clearance (C/T <0.1) behave like the axial flow impeller and generate a single-eight loop flow. This low-clearance range is the most efficient condition for the impellers (Sharma and Shaikh, 2003). Foucault et al. utilized the determination theory of just-suspended speed that was developed by Zwietering, using Delfo, Sevin and Hybrid coaxial mixers. It was shown that for Newtonian or Non-Newtonian continuous phases, the capability of Sevin and Hybrid impellers to generate axial pumping was better than Deflo and they needed lower N_{js} (Foucault et al., 2004). Bararpour et al. studied the power consumption and homogenization efficiency in a dual shaft mixer consisting of a wall-scraping Paravisc and Deflo disperser in the case of a highly viscous continuous phase. In their work, the power consumption by solid-liquid dispersion was detailed. They showed that Deflo provides good pumping capacity and increasing the rotational speed of the Deflo lowers the Paravisc power draw. They also explained the maximum and minimum power consumption by the possibility of the formation of particle agglomerates (Bararpour et al., 2007). Pinelli and Magelli studied the solid distribution in pseudo plastic fluid in a stirred tank with four Rushton turbines. They found out the concentration profiles of two different pseudo plastic liquids are qualitatively

similar with Newtonian liquid and the higher viscosity of the primary liquid makes the lower deviation from suspension homogeneity (Pinelli and Magelli, 2001). Fajner et al. studied the dispersion behavior of buoyant solid particles in multiple Rushton turbines. Due to the buoyant property, the solid concentration in this case is increasing from tank bottom to top, which is symmetrical to the profile of solid particles with higher density than continuous liquid. Moreover, the higher speed causes more uniform concentration distribution. They also pointed out that the solids loading has no effect on the concentration profile (Fajner et al., 2008). Kresta and Wood investigated the effect of the impeller clearance on the flow pattern generated by PBT in a fully baffled stirred tank. They concluded that by increasing the impeller clearance the angle of flow discharge from the axial direction toward the radial direction will be changed (Kresta and Wood, 1993). Hicks et al. studied solid suspension with four-bladed, 45° pitched blade turbines and Chemineer high-efficiency impellers. They reported that impeller type and physical properties do not strongly influence cloud height except for the fastest-settling solids (Hicks et al., 1997). Peker and Helvaci also reported that the degree of homogeneity decreases when the terminal velocity of the solid particles increases (Peker and Helvacı, 2007). A similar trend was also observed by Godfrey and Zhu (Godfrey and Zhu, 1994). Hoseini et al. investigated the effect of impeller type (LightninA100, A200, A310, and A320impellers), impeller speed, impeller off-bottom clearance, particle size (210–1500 mm), and solid concentration (5–30wt %) on the degree of homogeneity in an agitated tank. They developed CFD modeling to explore the effects of these parameters on mixing and compared their results with the experimental data. It was shown that the homogeneity of the system will be increased by increasing impeller power/speed. When homogeneity reaches the maximum, any further increase in impeller power/speed is not beneficial, but detrimental. The reason is the formation of regions with low solid concentrations inside the circulation loops at higher impeller speed. Hence, in a solid–liquid mixing system, the measurement of the optimal impeller speed as a function of the operating conditions and design parameters has a vital role in achieving maximum homogeneity (Hosseini et al., 2010a, Hosseini et al., 2010b). Tamburini et al. employed CFD modeling to investigate the dynamic behavior of the mixing of the silica suspension in a fully baffled mixing tank equipped with a radial flow impeller (Rushton turbine). They observed a high level of agreement between experimental results and relevant computational pictures (Tamburini et al., 2009). Ochieng et al. investigated nickel solids distribution with a four blade hydrofoil propeller in a stirred tank, using CFD and experimental

methods. They reported that for high solids loading, the turbulent dispersion force is very important. By increasing particle size and loading, axial concentration distribution decreases and the difference between axial solid concentrations at different elevations increases (Ochieng and Lewis, 2006a, Ochieng and Lewis, 2006b). Fradette et al. employed CFD modeling to explore the migration of particles in a stirred vessel and developed the diffusion model to predict the behavior of concentrated suspensions. The average behavior of a suspension in a three dimensional situation can be predicted with this model (Fradette et al., 2007a).

1.3.1. Maxblend Impeller

In the 1990's, a wide impeller named Maxblend was designed by Sumitomo Heavy Industrials (SHI) Mechanical & Equipment. It combines two parts, a low paddle and a grid. The Maxblend is one of the most promising impellers of the new generation, due to its good mixing performance, its low power dissipation, its simple geometry that makes it easy to clean, and its capability of operating in a wide range of Reynolds numbers (Mishima, 1992, Kuratsu et al., 1995).

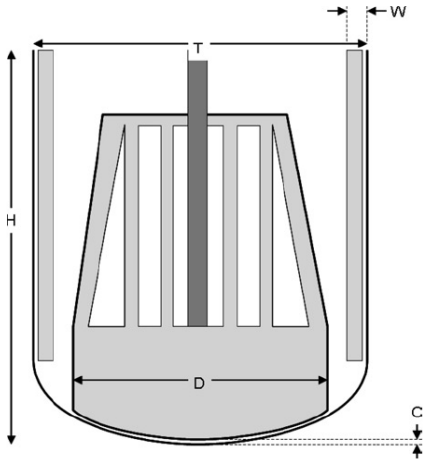

Figure 1-6: Schematic of the Maxblend impeller

The Maxblend impeller represents an interesting alternative to close-clearance impellers and it has been used in different processes. SHI uses the Maxblend for a variety of applications in liquid-liquid, liquid-solid and gas-liquid mixing. According to the manufacturer claims, the

Maxblend can handle processes from suspension polymerization and crystallization operation to high viscosity gas absorption. The Maxblend design idea originally comes from multi-stage impellers. As shown in Figure 1-7, the separation plan (interfering boundary) is formed by the upward and downward flow while the two multi-stage impellers are rotating. By combining the two impellers in a wide impeller, the boundary can be eliminated. Moreover, moving the impeller close to the bottom of the tank creates just one circulation flow in the tank. Finally, by adding the grid part, efficient mixing can be achieved. In addition, the simple shape of the impeller (no pitch, no angle, no spiral) makes the clean-up process easy and reduces the adhesion problem and the polymer blocks.

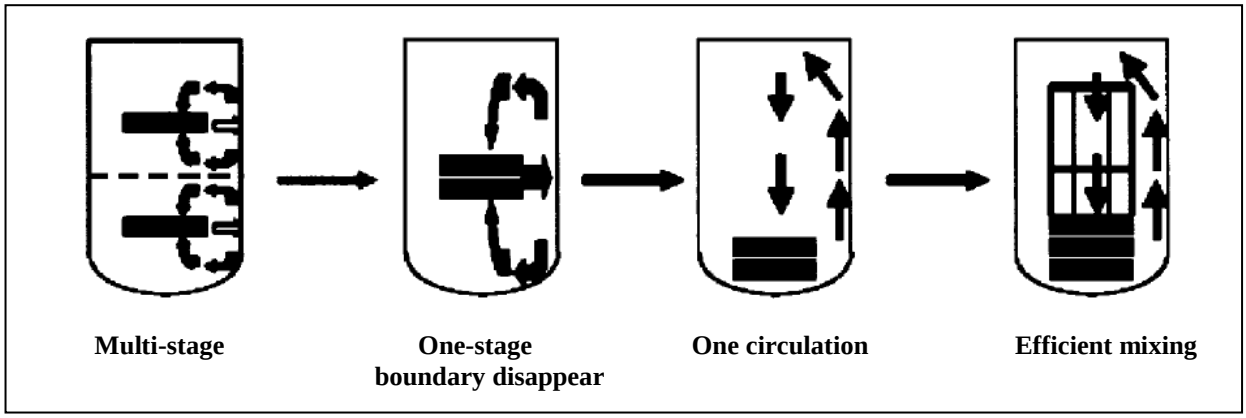

Figure 1-7: Concept of the Maxblend design (Iranshahi et al., 2007)

The top-to-bottom pumping induced by Maxblend is remarkable: the flow goes upward near the wall and downward in the center along the shaft. With regard to the flow pattern in the Maxblend mixer, it was proven that the paddle produces a strong tangential flow and a weak axial flow, generating a strong recirculation at the bottom of tank that causes flow segregation, while the grid part generates an axial pumping, with an upward motion at the vessel wall and a downward flow along the shaft. Therefore, four large loops are generated in the tank, two near the paddle (one in front and one behind) and two in the grid region (Figure 1-8). In fact, due to the symmetry, these four loops comprise two mixing structures: one at the bottom and one at the grid part (Iranshahi et al., 2007). The size of the two bottom circulation zones decreases by increasing the Reynolds number (Devals et al., 2008).

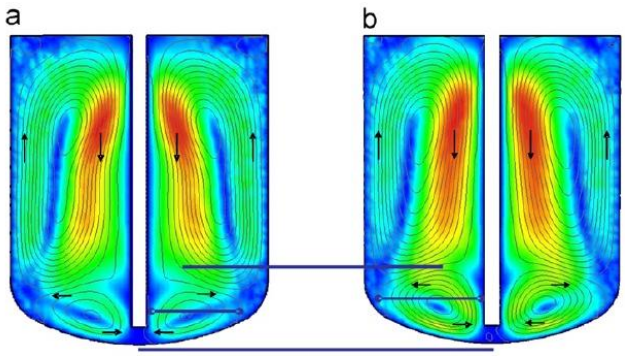

Figure 1-8: Effect of Reynolds numbers on flow pattern and velocity field for un baffled configuration: (a) Re = 80 (b) Re = 40 (Iranshahi et al., 2007)

There are different types of Maxblend, including: straight, wedge, modified N°1, and modified N°2, which are shown in Figures 1-9 and 1-10. The Maxblend modified N°1 presents small apertures accounting for 1/3 of the paddle surface and the Maxblend modified N°2 presents larger openings, about 2/3 of the bottom paddle surface. The shape of the Maxblend is known to influence the overall pumping capability. The wedge type is used for viscous applications while the straight-shaped Maxblend is preferred for the turbulent regime. The recirculation areas observed in high viscosity with the wedge Maxblend can be removed by making openings in the bottom paddle.

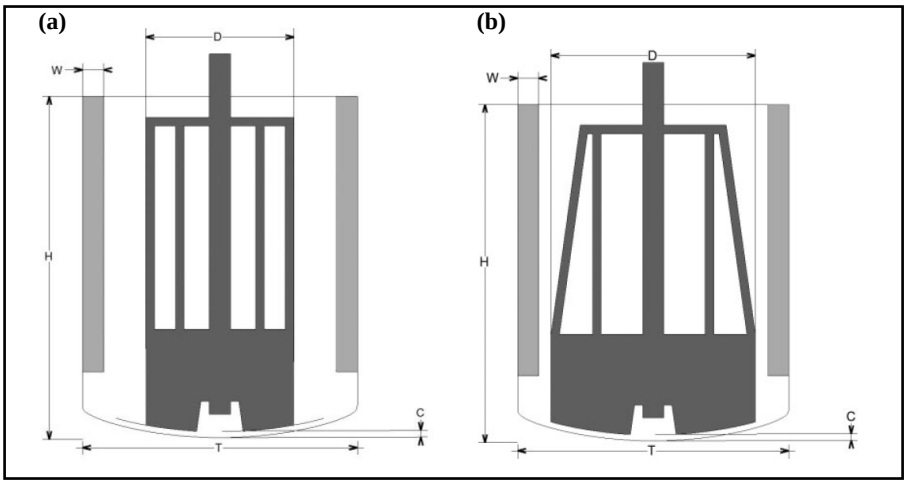

Figure 1-9: (a) Straight Maxblend impeller (b) Wedge Maxblend impeller

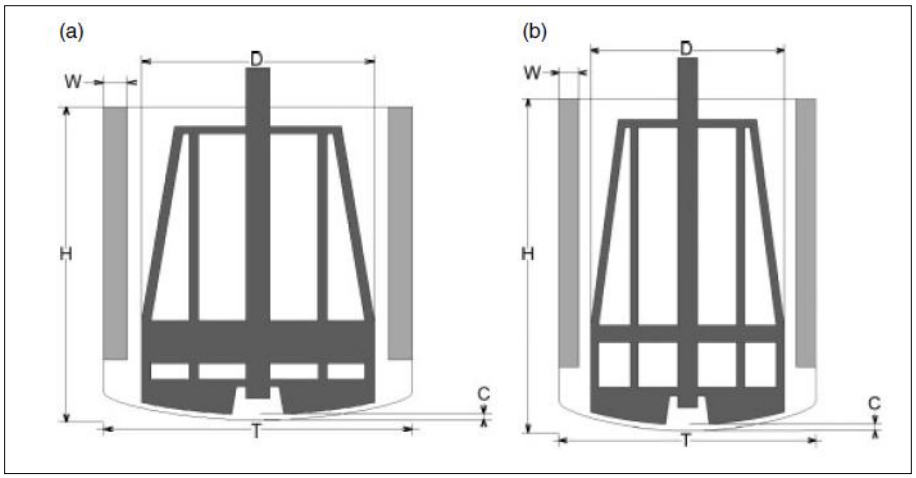

Figure 1-10: Maxblend modified (a) N°1 and (b) N°2

The Maxblend impeller represents an interesting alternative to close clearance impellers. However, little information is available to understand and explain its good performance in many difficult mixing processes. Yao et al. carried out a numerical investigations on dispersive mixing involving the Maxblend and a comparison with double helical ribbon impellers indicates that the Maxblend exhibits satisfactory local dispersive mixing performance (Yao et al., 2001).

The double helical ribbon impeller is unable to generate local mixing, although it can induce efficient global circulation throughout the stirring tank (Fuente et al., 1997).

Fradette et al. carried out a comprehensive investigation on the mixing characteristics of Maxblend in terms of power consumption, mixing evolution and mixing time in the laminar, transient and turbulent regimes with both viscous Newtonian and Non-Newtonian fluids in three different setup scales (Fradette et al., 2007b). For Newtonian fluid it was found that the regime becomes transitional from Re =40 and 50 with and without baffles. The turbulent regime starts at Re=300. For the Non-Newtonian fluid the trend is different. The laminar regime seems to be finished at Re=3 for both baffled and unbaffled conditions, but in the extended part there is a rapid and linear decrease at Re=10 for unbaffled mode and an obvious transition curve for baffled condition. Moreover, the power consumption for both Newtonian and Non-Newtonian fluids is the same in this mode.

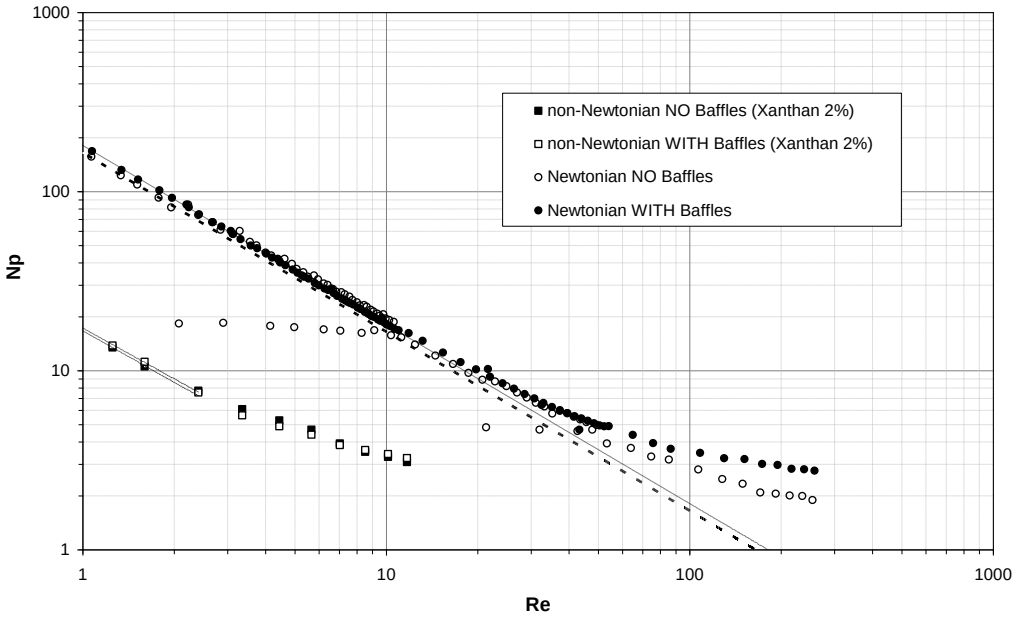

Figure 1-11: Power curves for Newtonian and non-Newtonian fluids, Maxblend 35 L (Fradette et al., 2007b)

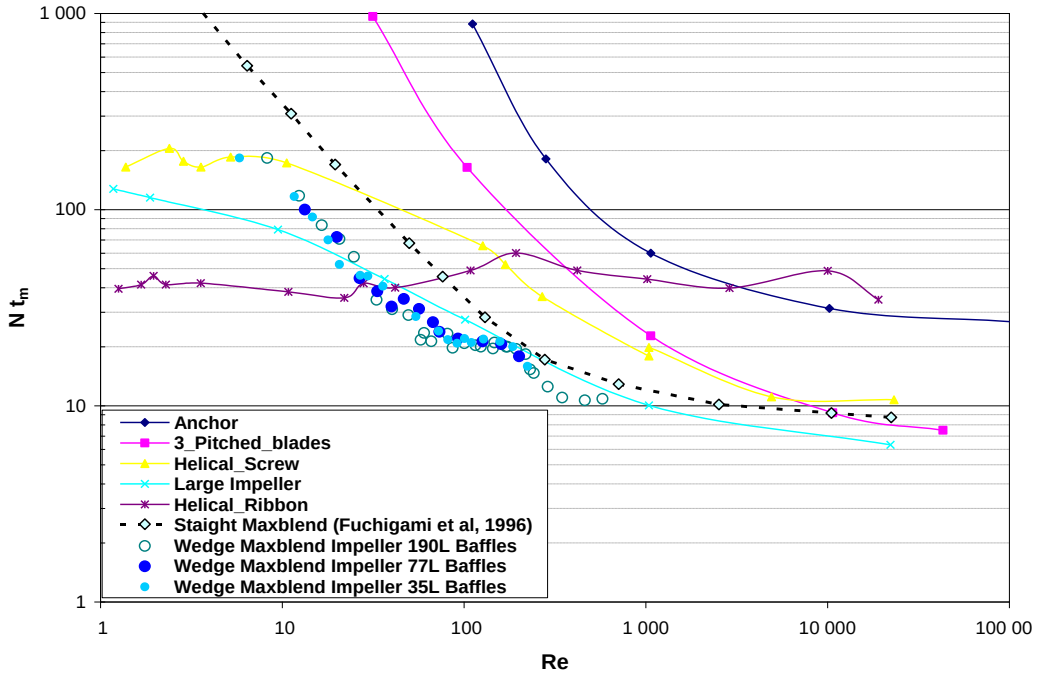

Figure 1-12: Comparison of various mixing agitators based on the dimensionless time (Fradette et al., 2007b)

They also studied the mixing time and power consumption of two types of Maxblend comparing with other large impellers. As it were shown in Figures 1-12 and 1-13, the Maxblend performs

advantageously in the range of Re larger than 20–30. At lower values, the HR takes over and at larger values, the Maxblend is comparable to the best geometries. For power required for mixing, the comparison with the same impellers shows again reveals a good performance of the Maxblend in the Re range larger than 0.1.

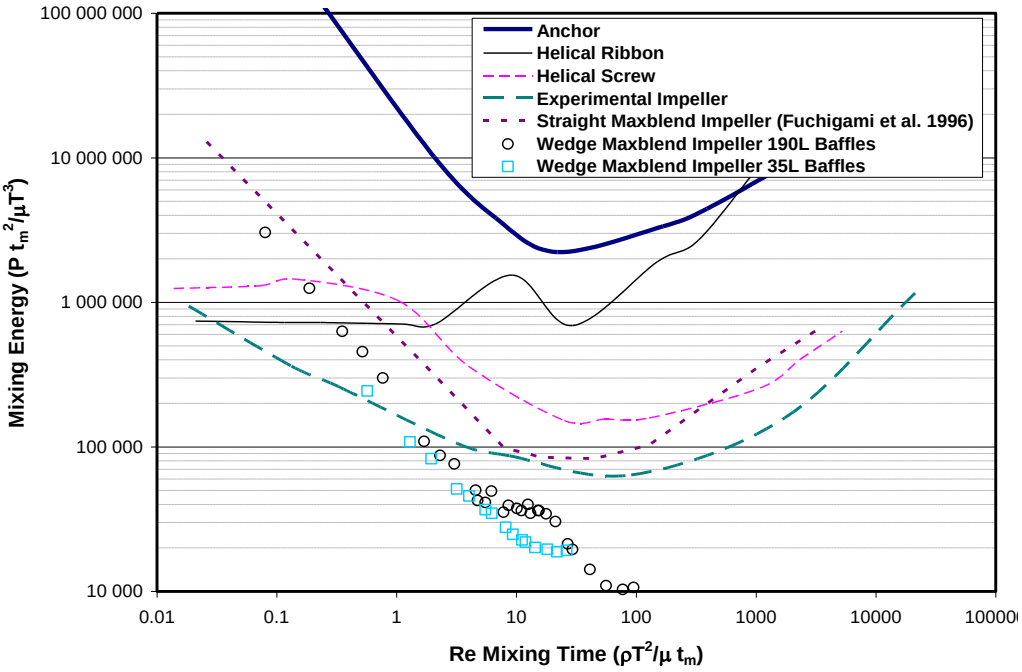

Figure 1-13: Comparison of various mixing geometries based on the mixing energy versus the Re mixing time. Data for agitators other than Maxblend taken from Yamamoto et al., 1998. (Fradette et al., 2007b)

Hiruta et al. investigated the application of the Maxblend fermentor for microbial processes and compared its performance with a turbine impeller fermentor. They concluded that the shear stress distribution for the Maxblend is more uniform than the turbine impeller (Yamamura and Hiruta, 1997).

Yao et al. carried out a numerical investigation on dispersive mixing of the Maxblend and compared it with helical ribbons impellers. They showed that even though the Maxblend has efficient performance at high Reynolds numbers, the dispersive mixing cannot be achieved at a deep laminar regime (Yao et al., 2001).

Dohi et al. investigated the power consumption and solid suspension performance of the Maxblend and other large-scale impellers in a gas-liquid-solid reactor. They found that the

Maxblend has the minimum power consumption and the most uniform solid suspension among the large scale impellers (Dohi et al., 2004).

Sumi and Kamiwano studied some mixing characteristics of the Maxblend with highly viscous fluids and compare it with multistage impellers (Sumi and Kamiwano, 2001).

Takahashi et al. have investigated liquid phase mixing time in boiling stirred tank reactors for the maxblend and other large scale impellers. They found that the Maxblend has essentially the same performance as competing impellers in this application (Takahashi et al., 2006).

A numerical characterization of 3D mixing hydrodynamics of Maxblend highlighted that homogeneous mixing cannot be easily achieved for highly viscous fluid (Iranshahi et al., 2007).

Iranshahi et al. investigated the hydrodynamic characteristics of the Maxblend impeller with viscous Newtonian fluids. They carried out both laboratory experiments and CFD modeling. They showed that the best performance of the Maxblend mixer is achieved at the end of the laminar regime and in the early transition regime with baffles. The presence of baffles increases the axial pumping and the flow number. Also, they showed that in the Maxblend system the baffled configuration creates more shear rate variations in the tank. The interaction between the paddle edge and the baffle increases the shear rate by 30% compared to the unbaffled configuration. Compared with blade turbine impellers, the Maxblend has a very uniform shear rate distribution that makes it suitable for many shear sensitive processes. In addition, by increasing the Reynolds number the volume of the loops near the paddle diminishes (Iranshahi et al., 2007).

Gutzburger et al. tried to characterize the effect of the vessel geometry (number of baffles) and the shape of the Maxblend impeller (a modified configuration of the bottom paddle and the angle of the upper grid) on viscous Newtonian fluids. It was shown that the shape of the Maxblend influences the overall pumping capability. Modified geometries avoid the creation of unmixed volumes because of the destruction of the segregated zones at the bottom of the tank while they utilize the same mixing energy as the standard wedge Maxblend. Regardless of the flow regime, the number of baffles does not have a significant effect on the power consumption and the mixing time. They recommended using only 2 baffles for the industrial application (Guntzburger et al., 2009).

1.4. Measurement Techniques for Solid Distribution

There are many techniques available that can provide both qualitative and quantitative information on the solid suspension in the stirred tank. These techniques, either provide general observations and semi-quantitative information on the distribution of solids (visual observation, process tomography) or give accurate quantitative data on local concentrations of solids (conductivity probe, optical probe, sampling for external analysis, or process tomography) (Paul et al., 2004).

Visual observation: Visual observation is most commonly used to determine the minimum speed for the suspension of solids (N_{js}). Also, it is useful for roughly estimating the degree of homogeneity in a mixing tank. Observation is necessary in order to choose the best position for locating the instruments in the tank. It also helps us identify problems, such as stagnant areas where solids may collect. Despite the advantages of visual observation, this technique will not help in high solid concentration systems, because solids prevent most of the tank from being viewed. Visual investigation of mixing mechanisms may be possible at lower solid concentration, but flow pattern observations should be carried out at high concentrations due to the fact that flow patterns change considerably with solid concentration.

Conductivity probe: The conductivity probe is useful for obtaining precise and accurate information about local solid concentration. The dimensions of the measuring volume should be at least an order of magnitude greater than the dimensions of the solid particles, and the probe should allow free flow through the measuring volume. It is based on the conductivity changes in the suspension according to the quantity of present solid particles. The conductivity method is low cost and accurate in dense systems. But, there is an intrusive effect of the probe in the vessel. The influence of the probe on the suspension process can be eliminated by suitably adjusting the size proportion of the probe versus vessel diameter (McMillan et al., 1999, Nasr-El-Din et al., 1996, Spidla and Sinevic, 2005). Spidla et al. measured solid concentration by using a conductivity probe in a large scale vessel. They have also proved the presence of radial solid concentration in an agitated vessel (Spidla and Sinevic, 2005). Bourne and Sharma measured N_{js} from solid concentration change directly above the vessel bottom (Bourne and Sharma, 1974b) and Musil (Musil and Vlk, 1978).

Optical probe: Optical probes can also be used to measure solid concentration. Two types of optical probes exist, light absorption or light scattering. In both cases the amount of light absorbed or scattered is related to the solids concentration. This non-intrusive method is generally limited to solids concentrations less than 1–2%. This is due to the scattering and blocking of light by the solids between the source and the receiver.

Optical fibers also have been used widely for characterizing solid concentration in multiphase systems (Shamlou and Koutsakos, 1989, Magelli et al., 1991, Chaouki et al., 1997, Boyer et al., 2002)

Sampling: Direct sampling is a very useful method for cases where information about particle size distribution or solid concentration is required. Two methods exist for removing a sample from the tank: pump the sample out through a pipe, or take a grab sample. The removal of samples through a pipe should be performed isokinetically, meaning that the velocity of the sample, which enters the pipe, must be the same as the local fluid velocity, and the pipe must be aligned in the local direction of the flow.

Grab sampling is performed by means of immersing a container fitted with a lid into the tank. The lid is opened slightly in order to fill the container, then the lid is closed and the container is removed to withdraw the sample. This technique can be applied in many situations, as it can be done even at high solid concentrations. The major disadvantage of this technique is that the equipment is not commercially available. Thus, the required equipment has to be designed and built for each job. The sample withdrawal method is the simplest method and has been employed widely (Barresi and Baldi, 1987, MacTaggart et al., 1993).

Buurman et al. (Buurman et al., 1986) studied a highly concentrated system at relatively homogeneous conditions. They reported no differences in the solid concentration at three sample withdrawal points situated in an axial direction. Even though the presence of the radial concentration gradient depends on the agitator type and speed as well as on impeller off-bottom clearance, particle diameter and solid loading, the significance of it has never been analyzed in detail. Literature data suggest that the radial concentration gradients are usually negligible (Barresi and Baldi, 1987, Montante et al., 2002, Yamazaki et al., 1986). However, this assumption cannot be generalized. The presence of radial concentration gradients has been reported by Micheletti et al. (Micheletti et al., 2003). By measuring solid concentration at different radial positions they indicated that a solid concentration gradient exists and it depends

on impeller type, particle size and solid loading. It is negligible only for small particle sizes, but increases significantly when particles of a larger size or density are suspended.

Other techniques: To overcome the limitations and eliminate the subjectivity of these methods new techniques are proposed. Angst and Kraume determined axial and radial particle distributions using an endoscope system (Angst and Kraume, 2006). Micale et al. measured the N_{js} using pressure recording method. In this technique N_{js} is computed by measuring the change in the recorded pressure at the bottom of the vessel, while the impeller speed increases (Micale et al., 2000, Micale et al., 2002). Buurman et al. used the Doppler effect at the vessel bottom to measure N_{js} (Buurman et al., 1986). Chapman et al. studied N_{js} by measuring peak in solid concentration close to the bottom of the vessel (Chapman et al., 1983). Using radioactive tracer is another non intrusive method which has been employed by Rewatkar et al.. N_{js} is determined by monitoring the decrease of the rate of radioactive tracers, as the impeller speed increases (Rewatkar et al., 1991). Jafari developed a technique based on gamma ray densitometry characterizing N_{js} and he showed that this technique provides accurate measurements (Jafari, 2010).

Beside all these methods, Electrical resistance tomography is an emerging technology which is explained in detail in the next section.

Electrical resistance tomography (ERT): ERT is a nonintrusive measurement technique for obtaining information about the contents of process vessels. ERT can be used to investigate and monitor any process where the main continuous phase is at least slightly conducting and the other phases and components have differing values of conductivity. Multiple electrodes are arranged around the boundary of the vessel at fixed locations in such a way that they make electrical contact with the fluid inside the vessel but do not affect the flow or movement of materials. (Giguère et al., 2008)

The primary advantage of this technique is the realization of three-dimensional imaging in a solid-liquid environment. An ERT system contains a series of sensors, a data acquisition system, and an image reconstruction system which are shown in Figure 1-14. An ERT sensor consists of an array of electrodes (typically 16 electrodes) that are distributed along the inner periphery of a non-conducting tank at equal intervals (Figure 1-15). Each sensor follows a procedure, which is also known as data acquiring strategy, to collect boundary voltage measurements. A constant current of low frequency is applied to an adjacent pair of electrodes and the voltages measured

successively from each pair of adjacent electrodes. The current is then switched to the next pair and the voltage measurements are repeated. This procedure is repeated until a full rotation of electric field around the cross-section is completed.

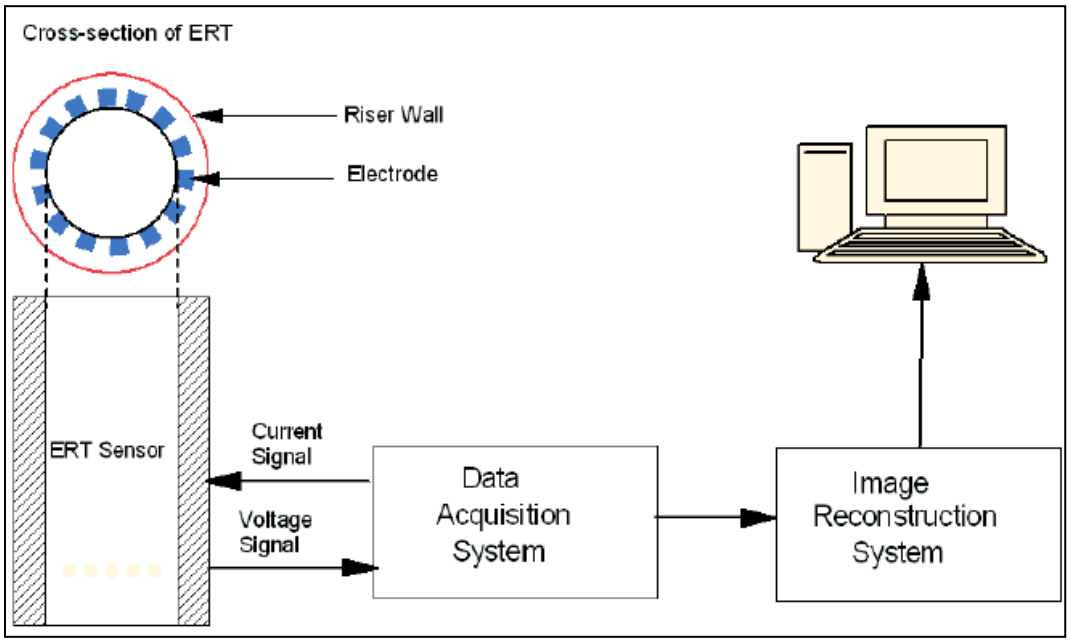

Figure 1-14: The schematic of ERT system

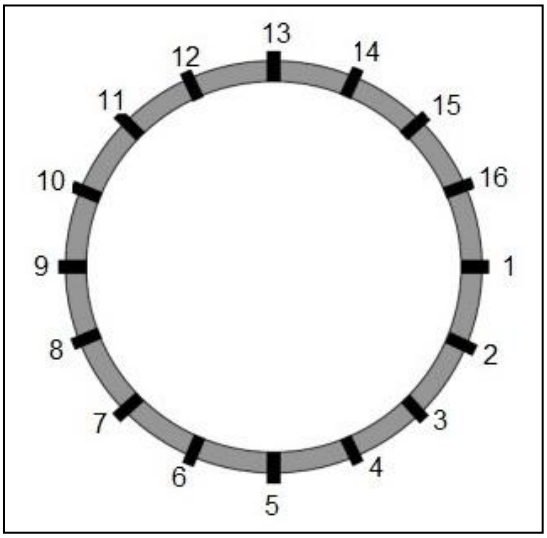

Figure 1-15: Schematic diagram of electrode arrangement and placement.(Xu et al., 2010)

Since the electrical conductivity for each electrode pair can be obtained, image reconstruction algorithms are used to compute a cross-sectional image. The Data Acquisition System is responsible for obtaining the quantitative data describing the state of the conductivity distribution inside the vessel. The data must be collected quickly and accurately in order to track small changes of conductivity in real-time thus allowing the image reconstruction algorithm to provide an accurate measurement of the true conductivity distribution. Finally, the solid and liquid concentration can be calculated and the concentration tomogram is able to display the situation of solid dispersion and distribution.

An ERT system produces a cross-sectional image showing the distribution of electrical conductivity of the contents of a process vessel from measurements taking at the boundary of the vessel. Figure 1-16 shows a typical tomographic image. The image contains a region of high conductivity indicated by the colour red and a region of low conductivity indicated by the colour blue. The scale below the image relates colour to conductivity. In this case the scale is between 0.08 and 0.15 mS/cm.

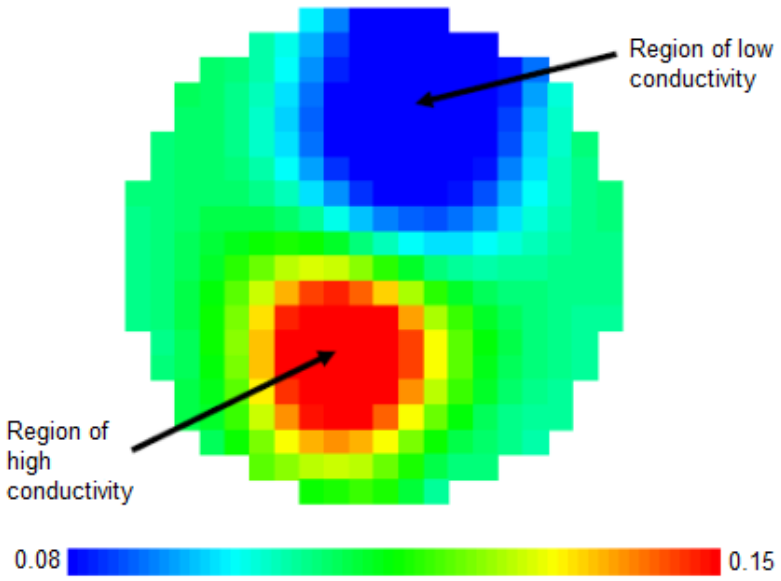

Figure 1-16: Tomogram showing region of high and low conductivity (ITS, 2009)

There is some literature reported on the ERT application in the stirred tank. Williams and Beck have discussed the difference of ERT technology from other tomographic approaches. They

proved that ERT measurement outperforms others on the faster data capture rate and finer spatial resolution (Williams and Beck, 1995).

Kim et al. studied a Rushton turbine mixing setup with two miscible liquids, tap water and brine. Data was collected on four virtual planes from top to bottom, called P1, P2, P3, and P4. Figure 1-17 demonstrates the relative conductivity measured by ERT, where darker shades of gray represent lower conductivity. Once the brine is injected into the tank, the top plane, P1, first displays the variation of conductivity in the center part. As the mixing continues, the darkness tends to even throughout the planes. Finally, when the local darkness disappears and the whole tomogram becomes uniform, the mixing process is considered to be finished (Kim et al., 2006).

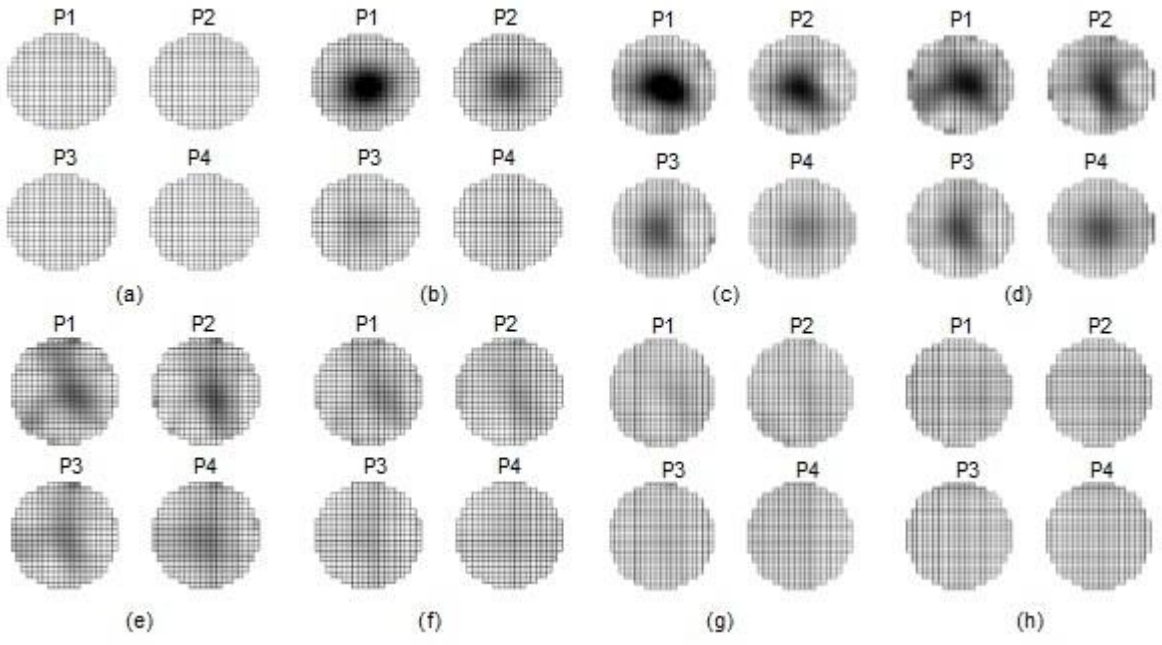

Figure 1-17: Tomograms of relative conductivity. (a) 40th frame, (b) 50th frame, (c) 60th frame, (d) 70th frame, (e) 80th frame, (f) 90th frame, (g) 100th frame, (h) 110th frame (Kim et al., 2006)

Hosseini et al. used ERT to investigate the solid–liquid mixing in an agitated tank equipped with a top-entering axial-flow impeller. The signals obtained from eight ERT planes were utilized to reconstruct the tomograms by using the linear back projection algorithm. The ERT measurements were correlated to solid concentration profiles by which the degree of homogeneity was quantified (Hosseini et al., 2010b).

While ERT has advantages in cost, speed and safety, it has its own drawbacks, including low resolution of reconstructed images and the measurement inaccuracy caused by the delay between particle dispersion and the time that signals are sent.

1.5. Summary and Objectives

In solid suspension process it is important to define what level of suspension is required versus the desired process results. While the just suspended condition is optimal for many processes, a high degree of suspension (homogeneity) is required for crystallization or the slurry feed system and partial suspension is sufficient for the dissolution of highly soluble solids. Failure to operate at optimal conditions leads to considerable drawbacks.

Choosing the proper impeller to satisfy the required solid suspension with a minimum power requirement is the key for the technical and economic viability of the process. Impeller plays several tasks in the agitation vessel; to suspend solid particles and to disperse them effectively. The flow pattern of axial flow impellers facilitates suspension in comparison to radial flow impellers. Many studies were done to find more effective impellers for solid-liquid suspension. Different Impellers, such as Lightnin A100, A200, A310 and A320, with high flow downward pumping were used in different studies. Cooke and Heggs reported that the hollow blade turbine is an efficient impeller for the solid-liquid mixing operations under gassed conditions (Cooke and Heggs, 2005). Bararpour investigated the dual shaft mixer consisting of a wall-scraping Paravisc and a high speed Deflo disperser (Bararpour et al., 2007). Lea employed a standard 45˚ pitch 6-bladed turbine (Lea, 2009) and Sardeshpande et al. used a down-pumping, pitched 6-bladed turbine (PBTD-6) and a 4-bladed Hydrofoil (HF-4) in their work (Sardeshpande et al., 2009). In most of these studies, tap water and glass beads (≤10%) were used. Several experimental methods such as visual observation, wall pressure fluctuation, laser-Doppler anemometry, densitometry technique and electrical resistance tomography were used to characterize N_{js}. These experimental techniques were applied to numerous empirical and semi-empirical investigations on solid suspension whose results were critically reviewed in the literature (for example (Jafari, 2010)).

The Maxblend is claimed to be one of the most promising impellers of the new generation, due to its good mixing performance, its low power dissipation, and its capabilities of operating in a wide range of Reynolds number. The Maxblend was designed for a variety of applications in liquid–liquid, liquid–solid and gas–liquid mixing. This recent product can handle processes from suspension polymerization and crystallization operation to high viscosity gas absorption.

However no experimental mixing characteristics on solid suspension with Maxblend are available in the open literature. Therefore, the objective of the present work is to determine the performance of Maxblend in producing solid suspension in Newtonian fluids.

The related specific objectives are:

1. To characterize the power consumption and determine the mixing time for solid-liquid suspension in a Maxblend impeller for various solid concentrations.
2. To characterize mixing performance for a Maxblend impeller by introducing a new parameter, *homogenization speed*, and the comparison of performance for various operation and design conditions.

CHAPTER 2
METHODOLOGY

This work is an experimental investigation on solid suspension in a mechanically agitated vessel using a Maxblend impeller. The study considers Newtonian viscous fluid as continuous phase. We are especially interested in the performance characteristics of the impeller and how they evolve when the impeller operates with various operating conditions.

2.1. Methodology

In this part the methodology of the experiments is presented. The experimental setup and the materials used in the experiments are explained. Finally the experimental strategy demonstrates how the specific objectives were satisfied.

2.1.1. Experimental Setup

The schematic of the mixing rig with its major components are shown in Figure 2.1. The system consists of a vessel with 0.379 m diameter and 0.598 m height. The tank volume is 37 L. The Maxblend impeller has a diameter of 0.255 m and is driven by a variable speed motor. The speed is controlled by a solid-state frequency controller, receiving a feedback signal from a speed encoder. In addition, the shaft is equipped with a torque meter to measure the effective power consumption of the impeller.

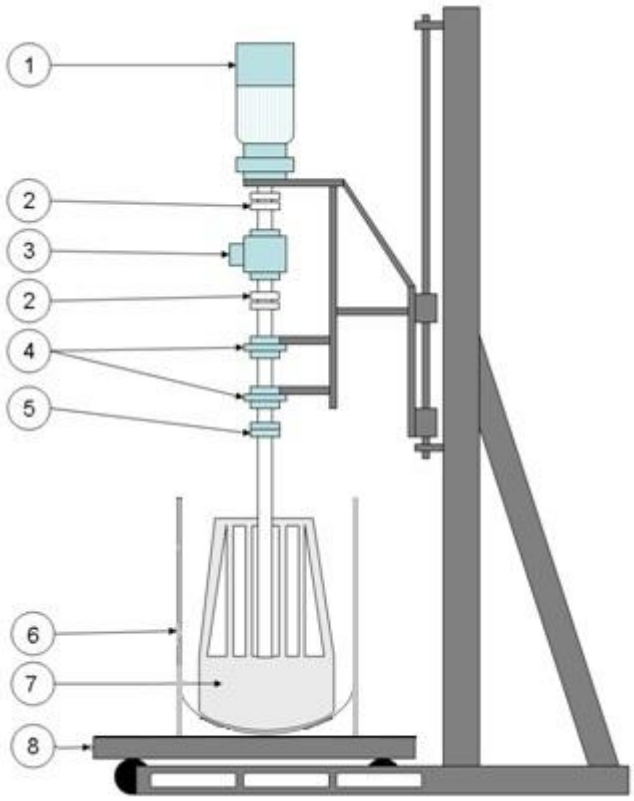

Number	Equipment
1	Motor and speed reducer
2	Torquemeter flexible couplings
3	torquemeter
4	Shaft bearings
5	Impeller flanged coupling
6	Polycarbonate vessel
7	Wedge Maxblend impeller
8	Transportation skid

Figure 2-1: Schematic of the mixing rig (Fradette et al., 2007b)

The geometrical details of the Maxblend set up are shown in Table 2-1. Two types of wedge Maxblend with flat and dish shape are used in this work (Figures 2-2).

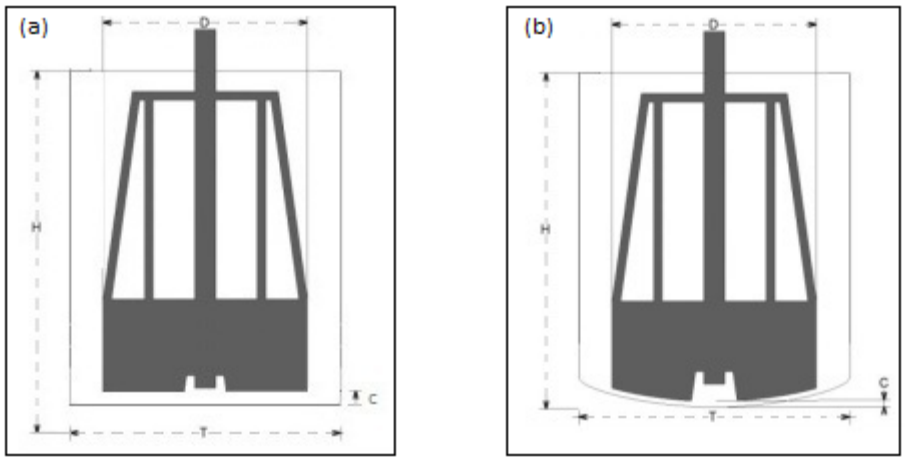

Figure 2-2: Wedge Maxblend impeller (a) Flat bottom and (b) Dish bottom

Table 2-1: Geometrical details of Maxblend systems

Mixing system	Tank dimension	impeller	Bottom clearance
Wedge Maxblend	T = 0.379 m H = 0.598 m V =37 L Material of construction: Plexiglass Geometry Cylindrical with flat /dish bottom	D = 0.255 m	C = 5.0 mm

The experimental set up used for the study is shown in Figure 2-3.

Figure 2-3: Photo of the experimental set up

2.1.2. Material

Tap water and glucose-water solutions were used in the experiments as the Newtonian continuous phase. Glucose-water solution is transparent with the viscosity varying from 0.1 to 13 Pa.s. Because the viscosity of the glucose-water solution is sensitive to temperature changes, process temperature was measured to correct the viscosity caused by temperature evolution.

A viscometer (Bohlin Visco88 and TA-Instruments AR2000) was used to determine the rheological properties of the solutions.

Glass beads were used as the solid phase with a density of 2.5g/cm^3 and nominal average size of 500 µm. Table 2.2 and 2.3 list the specifications of solid particles and liquid phase.

Table 2-2: Specification of solid particles

Shape	Nominal average size	Specific gravity
Spherical	500 µm	2.5 g/cm^3

Table 2-3: Specification of liquid phase

Liquid	Viscosity (pa.s)
Tap water	0.001
Solution of 90-98% glucose – water	0.1-13.0

2.1.3. Experimental Strategy

Throughout the experiments, we measure the power consumption and the mixing time in the Maxblend impeller as a function of various operating conditions.

The effective parameters on solid suspension which are investigated in this project are the design parameters, including the geometry of the tank bottom and the off-bottom clearance, as well as the operating parameters comprising the impeller speed, the solid concentration, and the viscosity of the suspending fluid.

To do so, we propose the following steps:

a) Characterization of the power consumption for Newtonian continuous phase and different solid concentrations in a Maxblend system.
b) Determination of the mixing time for solid-liquid suspension.
c) Characterizing the influence of design parameters (bottom clearance and bottom geometry) on the performance of Maxblend to reach uniform suspension. A new parameter, homogenization speed, will be considered for homogenous condition.
d) Characterization of the homogenization speed for solid-liquid suspension in a Maxblend mixer. The experiments will be carried out with different viscosities of continues phase and different solid concentration to verify the mixing efficiency of Maxblend.

The manufacturer recommended design value for bottom clearance in the liquid-liquid mixing is 5mm. During the experiments the dimensionless clearance ratio C/C0 was varied from 0.5 to 5.

2.2. ERT

ERT technology is used in order to measure and determine the solids dispersion state in the tank. Both qualitative and quantitative measurements can be carried out through the local conductivity of the liquid phase with the solids in the tank. The system contains 3 rows of 16 electrodes, each of which can be used for both excitation and voltage measurements. They are mounted flush at the tank wall. The primary function of the data acquisition system is to inject a current into adjacent electrode pairs and subsequently obtain the voltages on the rest of the others. This injection and feedback is repeated in sequence for all the electrode pairs until a full rotation of the electrical field is completed. The three levels are excited/read at the same time. Using the measured voltages at the electrodes, the electrical conductivity distribution on the cross-section is computed by means of an image reconstruction algorithm, and then the concentration of each phase can be calculated. The basic idea of colors in a tomogram is to reflect the conductivity and ultimately the solids distribution on across section corresponding to an electrode plane. In this study, the liquid phase (tap water, water-glucose solution) were conductive and the solid phase

(glass beads) was virtually non-conductive. In tomograms, the blue color indicates the lowest conductivity, hence the highest concentrations of solid particles.

An apparent problem in ERT is the noise created by the metal agitator. To overcome this problem we perform reference tests for each plane, with motionless and moving impeller. By subtracting a reference from the images of the corresponding plane, we reduce the noise effect in the results.

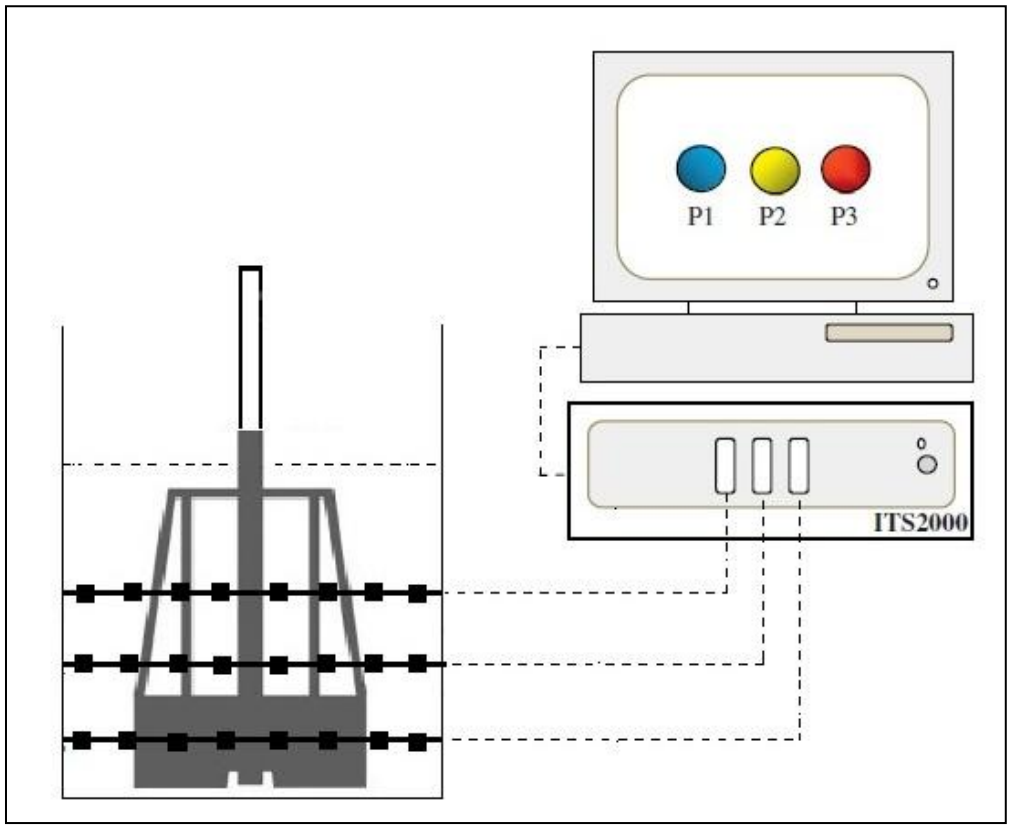

Figure 2-4: The schematic of ERT system

2.3. Power Consumption

Power consumption is determined by measuring the torque generated by the rotating impeller. Due to friction and other mechanical interferences, the residual torque obtained without fluid in the tank is subtracted from the measured torque to obtain the corrected torque used for power consumption calculations,

$$M_c = M_m - M_r, \tag{2-1}$$

where M_c and M_m are the corrected and measured torques, respectively. M_r is the residual torque. The power consumption can be calculated by the following equation

$$P = M_c 2\pi N, \tag{2-2}$$

where N is the impeller rotational speed.

2.4. Homogenization Speed

Although the just suspended speed (N_{js}) is an effective parameter for conventional impellers, it is difficult to apply with the Maxblend impeller because this impeller has small off-bottom clearance, and the particles could move on the bottom without being suspended. The suspending condition is completely different with Maxblend. Since the usual Zwittering criterion is not applicable, we propose to use a new parameter, the homogenization speed (N_H), as an indicator of uniform suspension. We define the homogenization speed as the speed at which a uniform suspension is reached. Homogeneous suspension is obtained when the particle concentration is constant within the tank. Once the homogeneity reaches the maximum, any further increasing in the impeller speed is not beneficial. The optimal impeller speed has a significant effect on the degree of homogeneity and should be always between two crucial impeller speeds, and the impeller speed for the maximum homogeneity, preferably closer to the latter (Hosseini et al., 2010b).

ERT technique is used to determine the homogenization speed (N_H) based on the distribution of the conductivity inside the mixing system.

2.5. Mixing Time

ERT provides conductivity and standard deviation data. Conductivity values describing the general behavior of mixture and the standard deviation specifies the mixing time.

In practice, since the axial lift velocity is small near the fluid surface, there is always a layer at the top with lower solid concentration, which prevents us from reaching 100% uniformity. As a result, obtaining a 95% homogeneity is often considered to be sufficient.

The time at which conductivity has less than 5% deviation from the final value corresponds to the mixing time. An example of typical mixing evolution curve is presented in Figure 2-5 along with the determination of the mixing time at 5% deviation.

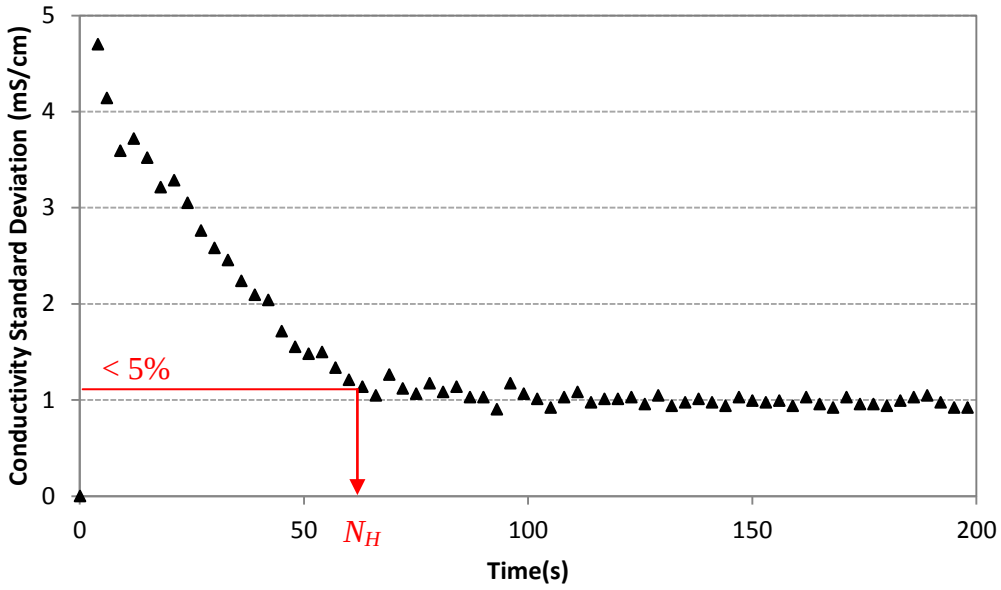

Figure 2-5: Typical suspending evolution curve (Tap water, v=5 wt%)

2.6. Reproducibility of experiments

To challenge the reproducibility of the method, the same experiments were repeated three times. These experiments were performed with tap water and 5 wt% glass beads. The impeller speed is 100 rpm. The results are reproduced in Figure 2-6 and present the normalized average conductivity of the tank depending on the frame number. Frame 0 corresponds to the starting time. From the figure, it can be seen that the results are very similar and lead to the same conclusion about the time to reach homogeneity.

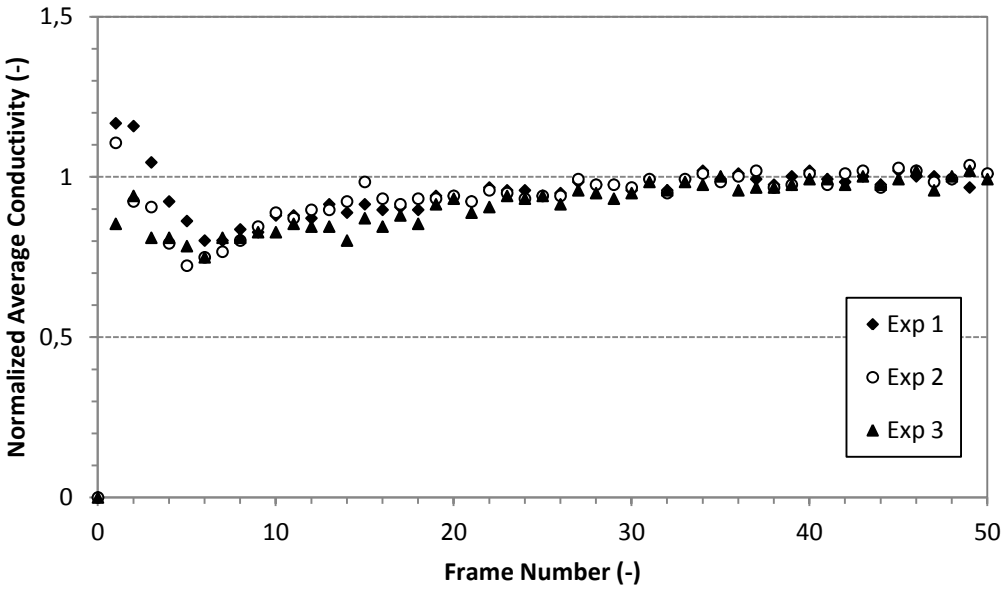

Figure 2-6: Reproducibility experiments, N=100 rpm (Tap water, v=5 wt%)

To be able to compare final conductivity levels from different experiments, we normalize the collected results.

Figure 2-7 presents the standard deviation from the final mean conductivity with the agitator rotating at 60 rpm as a function of the frame number. The curves overlap perfectly. Both figures 2-6 and 2-7 are useful for analyzing the ERT results. Conductivity values are describing the

general behaviour of solid suspension. N_H can be deduced by measuring the conductivity and the mixing time is verified by standard deviation.

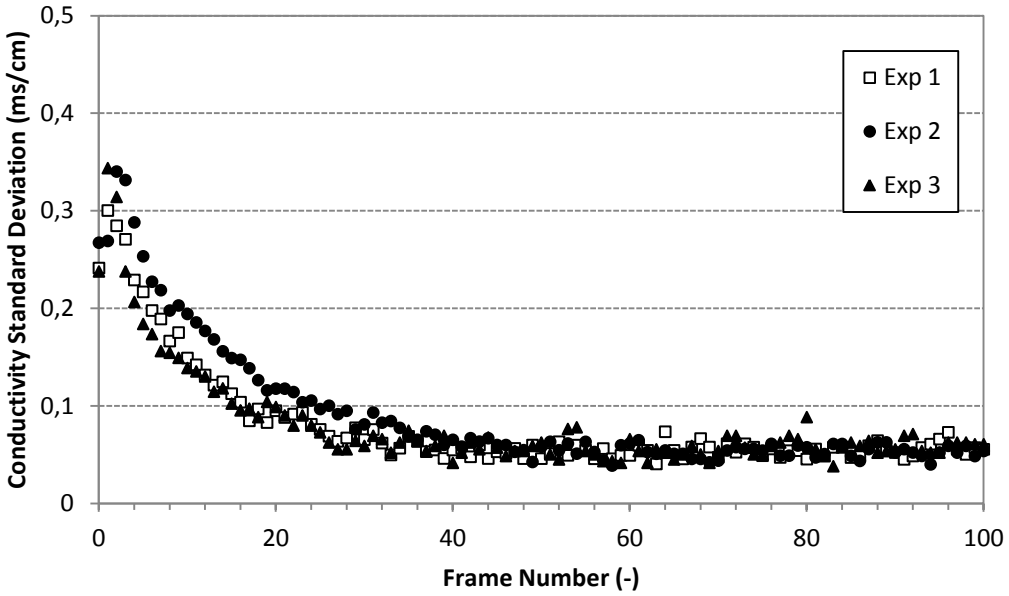

Figure 2-7: Reproducibility experiments, N=60 rpm (Tap water, ν=5 wt%)

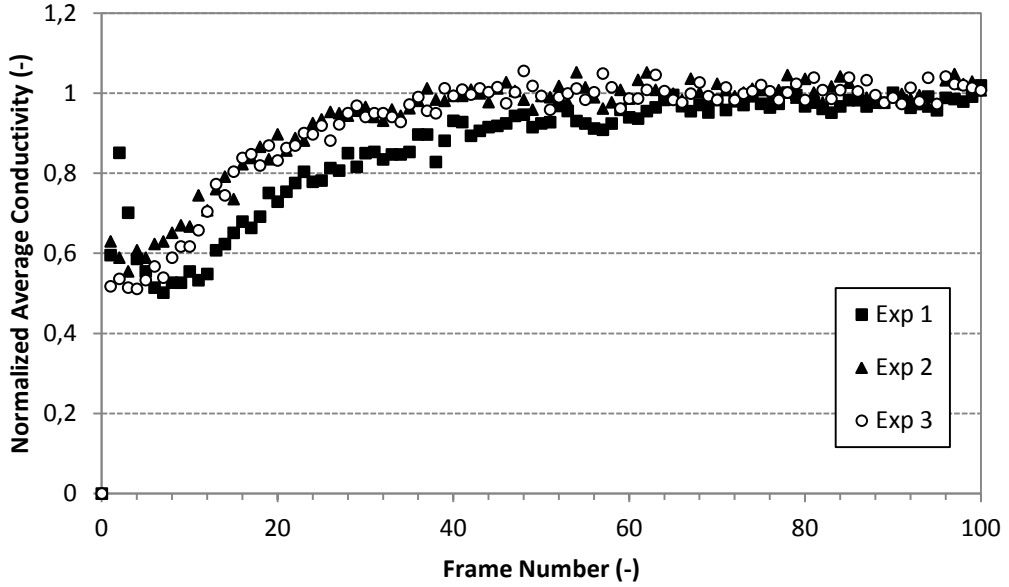

Figure 2-8: Conductivity curve at 60 rpm impeller speed (μ=0.1 Pa.s, ν=5 wt%)

The reproducibility of experiments for more viscous fluid was tested in three experiments with 80% glucose-water solution (μ=0.1 Pa.s) and 5 wt% glass beads (Figure 2-8). The results are successively reproduced. The three curves overlap to a great extent. This method has been confirmed to be usable for Newtonian fluids more or less viscous and its reproducibility was verified.

Figure 2-9 shows the normalized average conductivity of planes versus frame number for 60, 75 and 90 rpm respectively in 5 wt% glass beads. In constant solid concentration by increasing the impeller speed the suspension reaches the homogeneity faster.

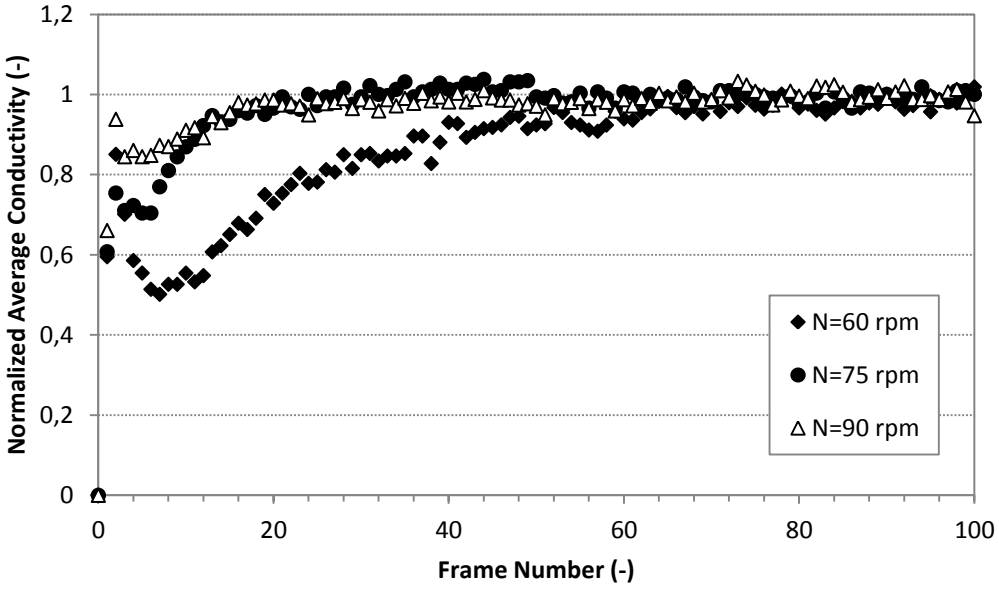

Figure 2-9: Conductivity curve for different impeller speed (μ=0.1 Pa.s, ν=5 wt%)

CHAPTER 3

RESULTS AND DISCUSSION

3.1. Solid Suspending Evolution

The evolution of the suspension homogeneity is shown on Figure 3-1. The Maxblend generates a

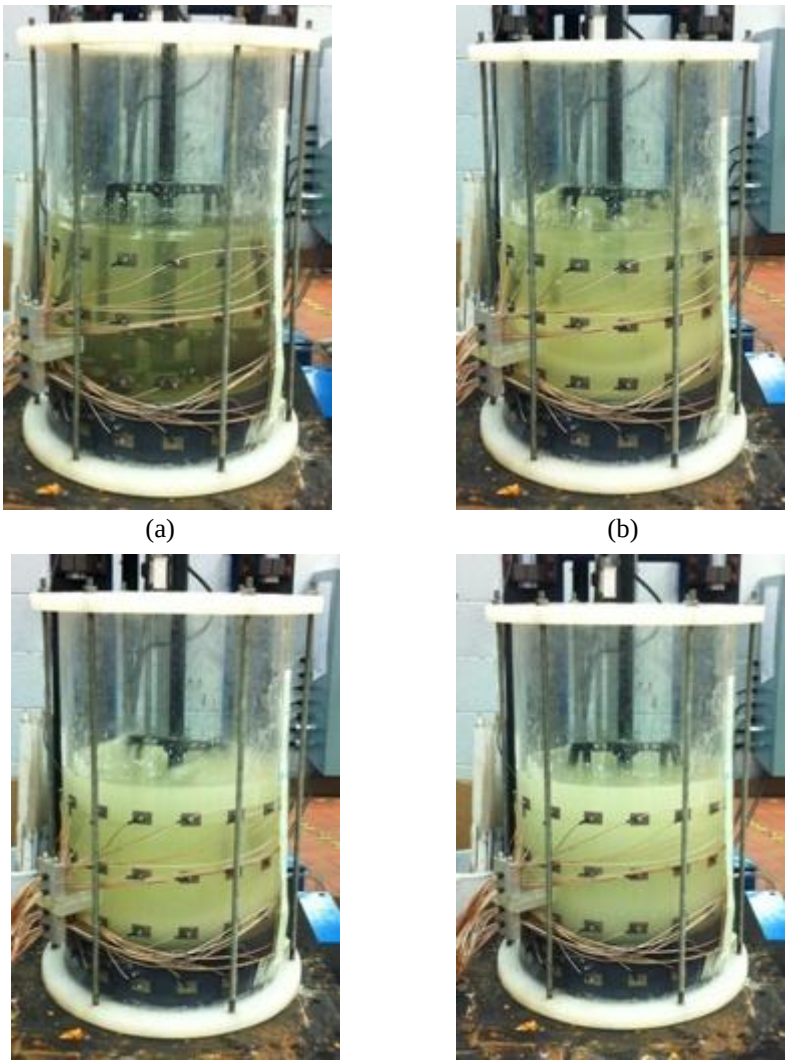

(a) (b)

(c) (d)

Figure 3-1: Solid suspending evolution with Maxblend

flow pattern which sweeps the tank bottom and suspends the solids. In solid suspension with the Maxblend, no interface between suspended layer and the clear liquid layer can be seen. This is caused by the strong up-pumping flow induced by this wide impeller, which makes it possible to yield a uniform solid suspending condition.

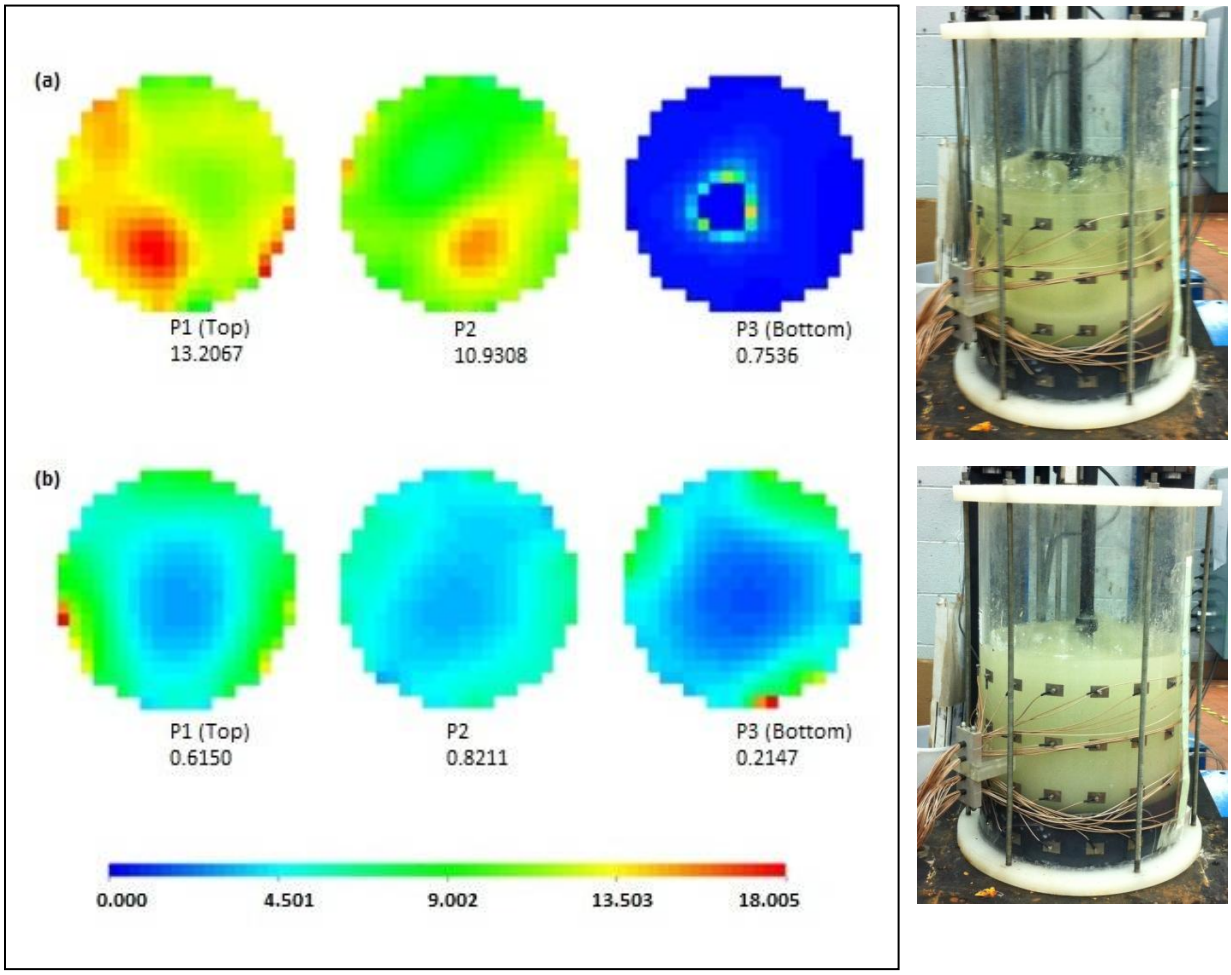

Figure 3-2: Tomograms obtained for the solid suspension at μ= 0.1 Pa.s, ν=5 wt%, dp=500μm: (a) N=40 rpm, (b) N=53rpm

Figure 3-2 displays set of tomograms for different condition of solid-liquid suspension for glucose solution and 5 wt% glass beads. Figure 3-2(a) shows an experiment carried out at N=40rpm (below N_H). At this impeller speed (below N_H) partial suspension was observed. This resulted in creation of three distinct zones: an unsuspended solids layer on the bottom (Plane 3), a clear liquid layer at the top of the vessel (Plane 1, P_1), and a region of solid suspension in

between (Plane 2, P_2). The blue region in plane 3 (bottom) indicates that most of the unsuspended solid particles rested on the bottom of the tank. It means all solid particles were not picked up by the fluid because of insufficient impeller speed. When the impeller speed was increased (Figure 3-2, b), solid suspension improved and the amount of solid particles that rested on the bottom of the tank decreased and eventually disappeared. The clear liquid layer in the upper region of the tank also decreased slowly and solid suspension reached its maximum homogeneity. This impeller speed was sufficient to suspend all solid particles and was considered as N_H.

The normalized average conductivity curve for this experiment is shown in Figure 3-3. By increasing the impeller speed, the amount of solid particles remaining on the tank base is decreased while the conductivity in this plane is increased. In addition, more solid particles disperse in the upper region of the tank and conductivity is decreased. Finally, we obtain uniform solid suspension.

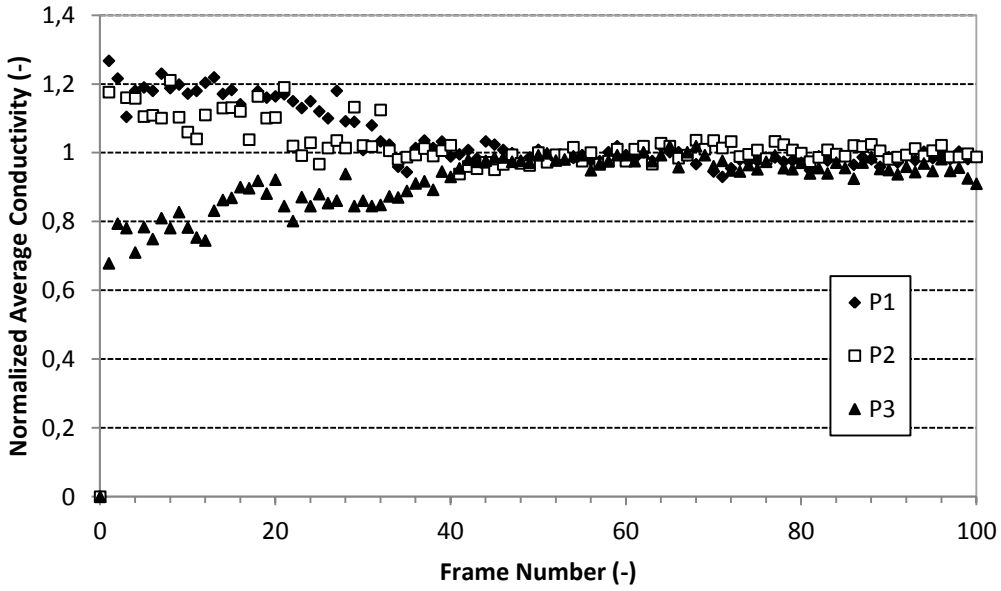

Figure 3-3: Normalized average conductivity curve for the solid suspension at μ= 0.1 Pa.s, ν=5 wt%, dp=500μm, NH=53rpm

3.2. Power Consumption

The experimental power curves for various solid concentrations are shown in Figure 3-4. We compute the power number and the Reynolds number using the Equations

$$N_P^* = \frac{P}{\rho^* N^3 D^5} \tag{3-1}$$

and

$$Re^* = \frac{\rho^* N D^2}{\mu}, \tag{3-2}$$

where ρ^* is the density of the suspension, which is defined as

$$\rho^* = \emptyset_v \, \rho_s + (1 - \emptyset_v)\rho_l. \tag{3-3}$$

In the absence of solid particles, for single phase the Maxblend impeller operates in the laminar region for *Re* lower than 50 and the regime becomes transitional from this point on, for Re higher than 300 the flow regime can be considered turbulent (Fradette et al., 2007b).

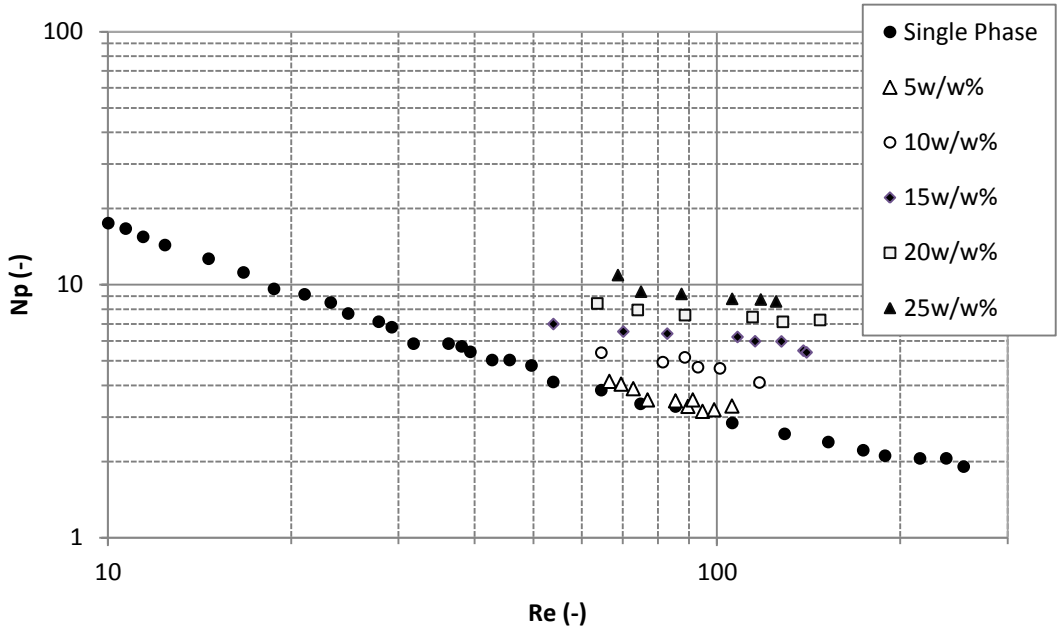

Figure 3-4: Power curves for single phase (Fradette et al., 2007b) and solid suspension (Glucose- water solution and glass beads)

As this figure reveals, the solid dispersion was performed in the transition region. For 5 wt% solid loading the power curve is above but close to that of a homogeneous liquid free of particles. This indicates that the modified equations taking the presence of the solid into account can handle low concentrations and the Np values obtained for the solid suspension can be considered as the same value. For larger solids loadings, Np is always higher with solids than for the single fluid. This can be interpreted as a modification of the viscosity that is not taken into account by the modified equations for Re and Np.

3.3. Mixing Time

The experimental dimensionless mixing times versus *Re* is presented in Figure 3-5. We observe that increasing the Reynolds number raises the pumping efficiency of the Maxblend axial motion and decreases the mixing time. Also, in presence of solids the mixing time increases, by a factor of 5 for 5 wt% solids, and a factor of 15 for 10 wt% solid particles.

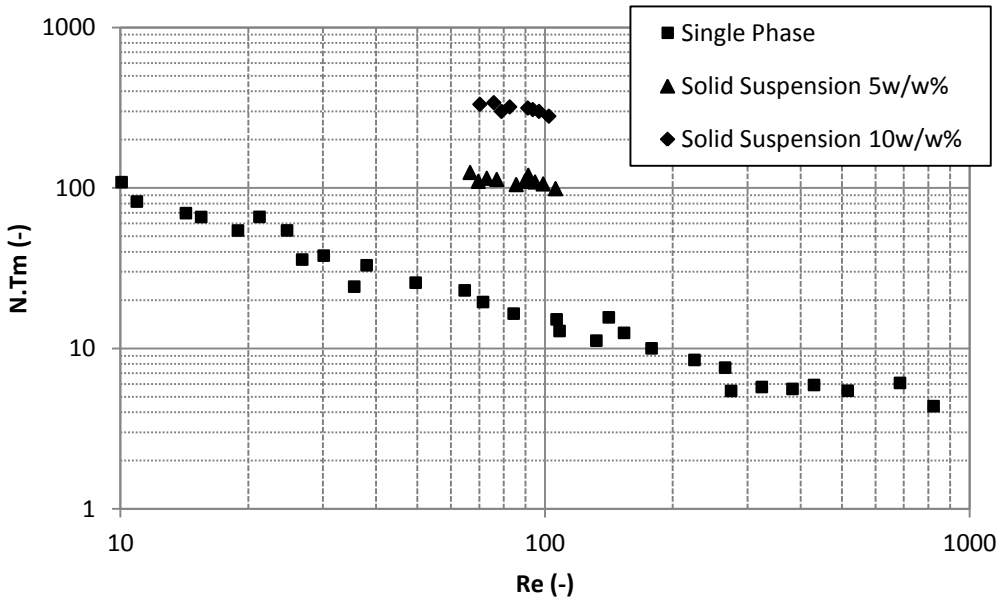

Figure 3-5: Experimental mixing times for a single fluid (Glucose- water solution) (Fradette et al., 2007b) and with solids present (5 wt%)

In the transient regime, the distributive motion is described as follows: the paddle is pumping the fluid through the tank, the fluid goes downward along the shaft and upward close to the wall. The grid part of Maxblend seems to force the fluid through this recirculation loop. Mixing is mostly achieved by axial pumping. Power consumption and mixing time can be explained with the dimensionless mixing time variations. The front side of the paddle at the bottom makes an overpressure and pushes the fluid close to the wall in the upward direction. The liquid at the top of the tank is sucked at the same time by the low pressure created at the tank bottom. The liquid goes downward along the shaft. The pressure drop generated by the paddle at the tank bottom is written as (dimensional analysis)

$$\Delta P \propto \rho V^2, \tag{3-4}$$

with ρ the liquid density, V the velocity written $V = ND$, N the rotational speed and D the impeller diameter. The downward flow rate (Q_z) is proportional to the pressure drop ΔP,

$$Q_z \propto \Delta P. \tag{3-5}$$

The mixing time T_m is proportional to the reciprocal of Q_z,

$$T_m \propto \frac{D^3}{Q_z}. \tag{3-6}$$

Therefore the dimensionless mixing time can be written as follows:

$$NT_m \propto \frac{1}{Re}. \tag{3-7}$$

Consequently, NT_m for Newtonian fluids decreases with the reciprocal of *Re*.

3.3. The Effect of Vessel Geometry

The shape of the vessel base, affects the location of dead zones or regions where solids tend to accumulate. It also influences the minimum agitation speed required for suspending all the particles from the bottom of the vessel. In flat-bottomed vessel fillet formation tends to occur in the corner between the tank base and the tank wall. In dish-bottomed vessel solids tend to settle

beneath the impeller or midway between the center and the periphery of the base. As illustrated in Figure 3-6, the homogenization speed (N_H) is 10% to 15% higher in a flat-bottomed vessel than a dish-bottomed one. This curve was obtained with 5-25 % solids in both cases. Figure 3-7 compares the power for suspending solids in flat and dish bottomed vessels. Not surprisingly, the power draw appears higher for flat-bottomed compared with dish-bottomed geometry.

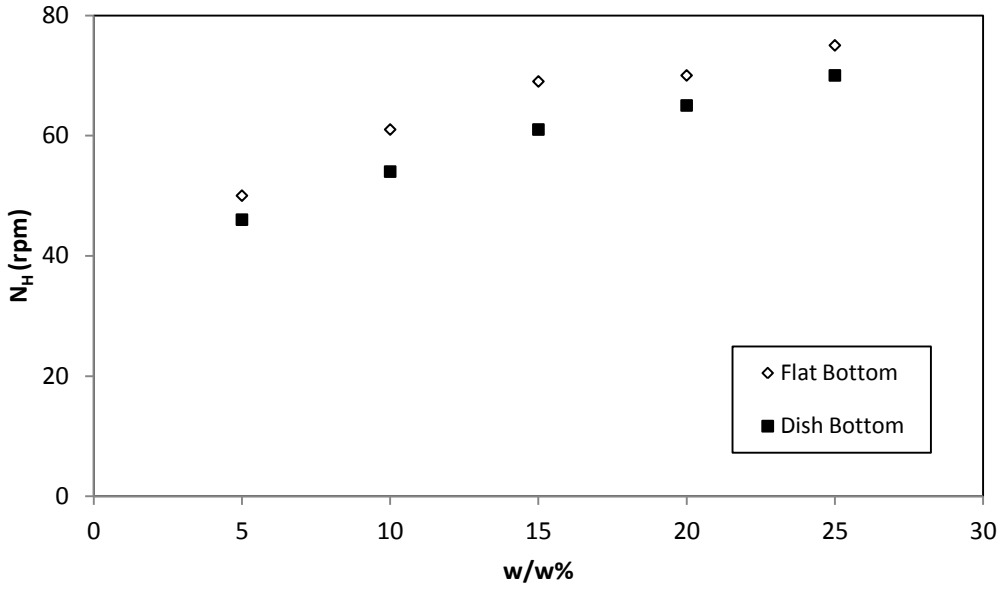

Figure 3-6: The effect of bottom geometry on N_H (glucose-water solution, μ= 4.78 Pa.s , v=5-25 wt%)

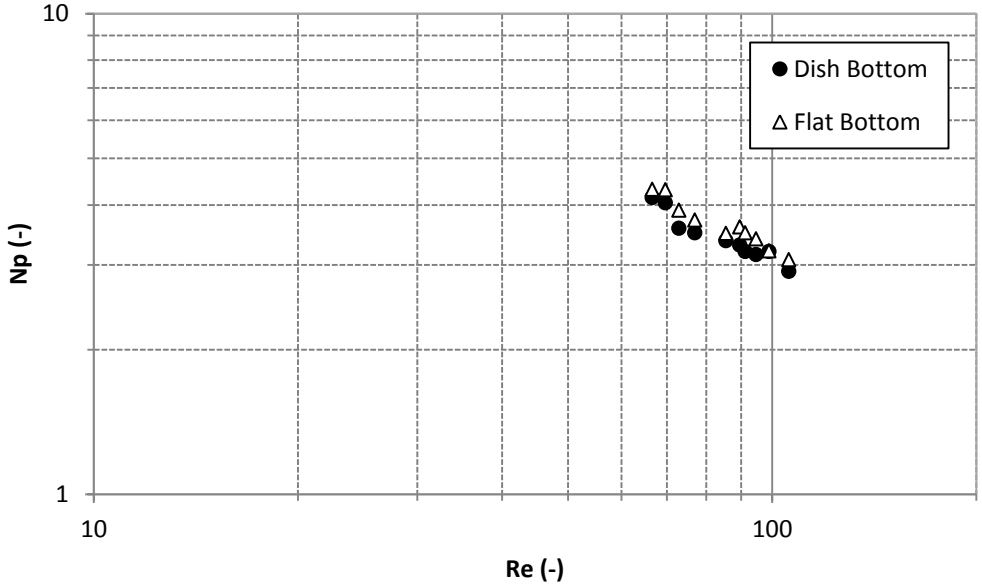

Figure 3-7: Power curves for 5wt% solid suspension in flat and dish bottomed tank

3.4. The Effect of Impeller Bottom Clearance

Impeller off-bottom clearance plays an important role in solid suspension. In configurations where the impeller operates close to the tank base, momentum transfer from the impeller to the particles is maximized. Under this condition, the particles trapped at the bottom of the vessel under the impeller are driven toward the junction of the tank base and wall. This motion faces minimal resistance while accumulating sufficient momentum to lift the particles into suspension after sliding toward the junction of wall and vessel base. By increasing impeller bottom clearance, the stagnant zone below the impeller increases and more solid particles are left in that region. Also, momentum transfer to solid particle decreases and higher impeller speed is required to force particles to move outward at the impeller periphery from where they are suspended. The effect of bottom clearance on N_H has also been investigated for flat and dish bottomed vessels, as, according to the manufacturer, the magnitude of the clearance can have a noteworthy influence on the mixing efficiency. Figure 3-8 shows the evolution of N_H versus C/C0, where C0 is the manufacturer recommended design value for the liquid-liquid mixing.

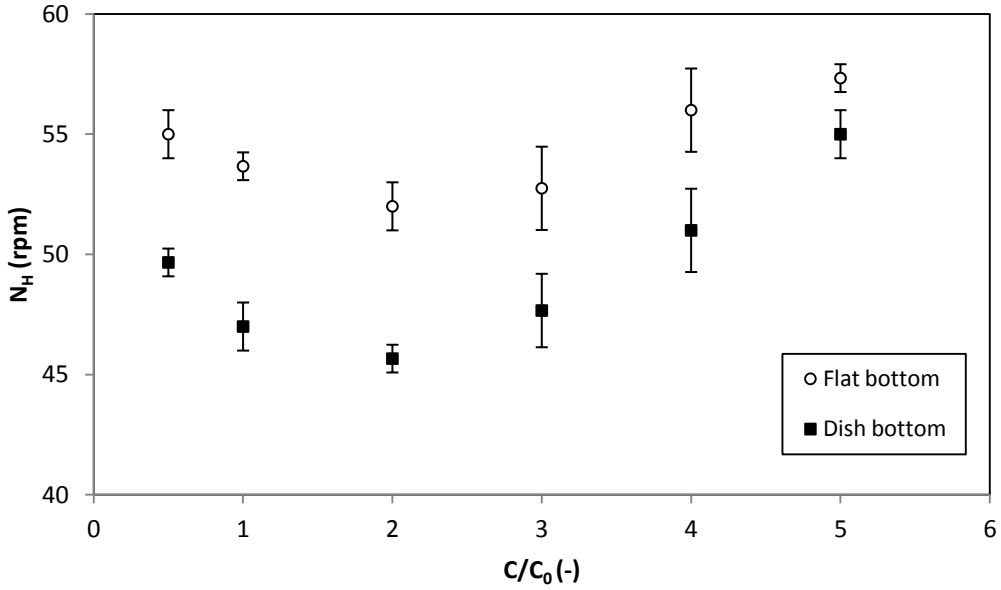

Figure 3-8: Effect of bottom clearance on the N_H (Tap water and glass beads, v=5 wt%)

The results shown here indicate that the bottom clearance might have a significant impact on the pumping capacity. It can be seen that N_H varies non-linearly with the clearance value. Small variations of the bottom clearance do not affect the mixing efficiency. The lowest N_H was achieved at C/C0=2. This clearance allows dissipation of segregated zones. It seems that no segregated zone exist for this value.

3.5. The Effect of Solid Loading

The effect of solid concentration on N_H, which is a crucial operating condition in solid–liquid mixing processes, was also investigated with 94% glucose solution as the continuous phase. As shown in Figure 3-9, higher solids loading causes an increase in required N_H. Upon increasing solids loading, more power is required to suspend large portions of solid.

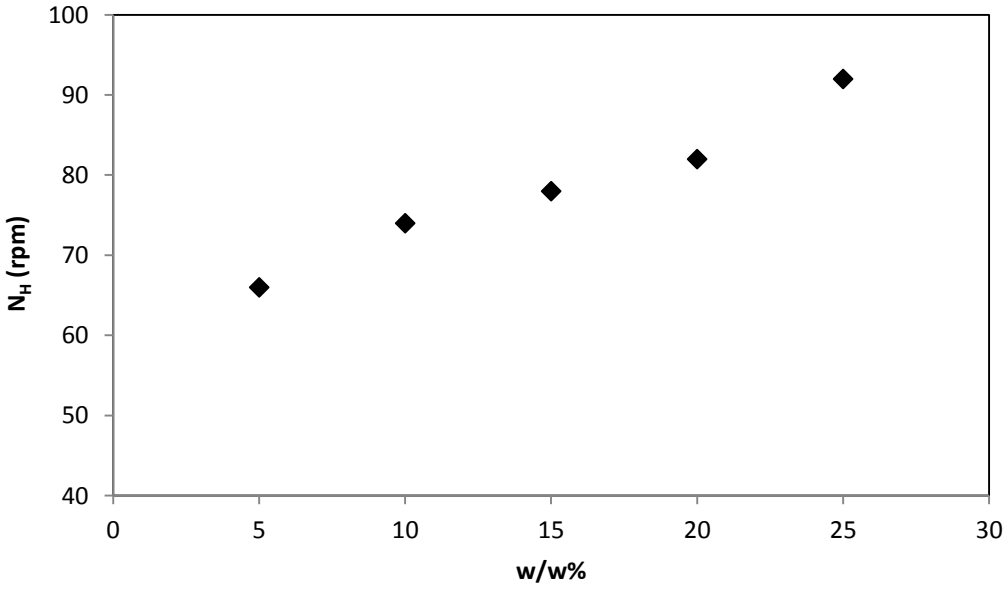

Figure 3-9: Effect of solid concentration on N_H (glucose-water solution, μ= 4.78 Pa.s, 58<Re<83)

The homogenization speed is related to the settling velocity of a particle, and the settling velocity is related to the concentration. Therefore, theoretically N_H changes with the solid concentration.

The graph clearly demonstrates this relationship. Solids loading can be expected to influence the impeller performance by modifying the suspension viscosity, local density and/or vortex structure in the vicinity of the impeller blades. In fact, when we increase the solid concentration, the apparent viscosity and density are increased, so the energy used by the impeller is dissipated without producing enough mixing in the tank hence higher impeller speed (more power) is needed to homogenize the system.

3.6. Solid Suspension in Viscous Fluid

The Maxblend impeller is one of the most efficient impellers to handle solid suspension in viscous fluids. The distributive motion makes the uniform suspension. The paddle is pumping the fluid through the vessel, the fluid goes downward along the shaft and upward close to the wall. The grid part of the Maxblend drives the fluid through this recirculation loop. Mixing is mostly achieved by axial pumping and this flow pattern sweeps the tank bottom and suspends the solids.

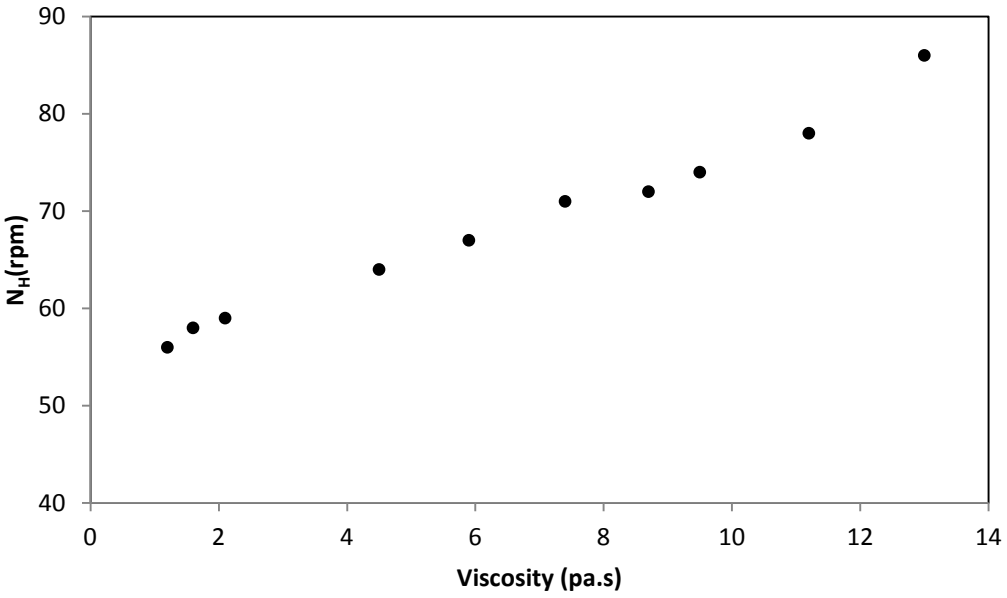

Figure 3-10: Effect of liquid viscosity on N_H (glucose-water solution and glass beads, v=5 wt%)

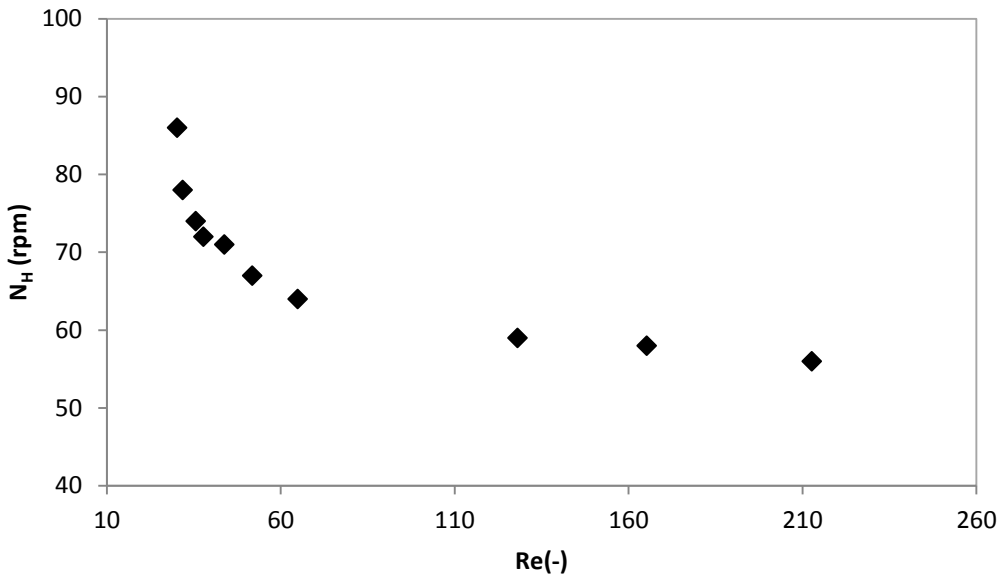

Figure 3-11: Homogenization speed curve (glucose-water solution and glass beads, v=5 wt%)

The N_H for different viscosity is shown in Figure 3-10, for the solution of 5% - 92% of glucose. The results demonstrate reaching uniformity by Maxblend in high viscosity. It can be seen that increasing liquid viscosity, causes an increase in N_H. It means that for lifting the particles in higher viscosity more speed hence more power is required.

Figure 3-11 presents N_H versus *Re,* allowing for the simultaneous analysis of N_H and the mixing time. We observe a trend similar to that of the master power curve (*NP* vs. *Re*).

3.7. Comparison of ERT with the Sampling Technique

Results of the ERT technique were compared with a sampling technique in Figure 3-13. For local solid concentration measurement, the slurry solution is sampled by suction from the upper, middle and lower part of the vessel. Sampling points were along the vessel wall. At several power inputs the necessary impeller speed to reach the uniform suspension are estimated by sampling data. ERT is a novel technique to image the electrical conductivity distribution in a cross-section by applying currents at the boundary and measuring the resulting voltages.

As illustrated in Figure 3-13 the sampling technique underestimates the homogenization speed compared to the ERT technique. These differences in N_H values obtained using the different methods do not exceed 25%. However, there are several reasons why ERT technique is more accurate. First, sampling has been carried out at only 3 points and the data from these sampling points are not rich enough to characterize the particle concentration profile in the whole vessel. Also, an accurate measurement requires the velocity of the sample entering the pipe to be the same as the local fluid velocity, and the pipe to be aligned in the local direction of the flow. The difficulty to obtain these conditions in practice leads to more imprecision.

In addition, ERT is a non-intrusive method and has advantages in cost, speed and safety. Nevertheless, it has its own drawbacks, including low resolution of reconstructed images and the delay between particle dispersion and the time that signals are sent.

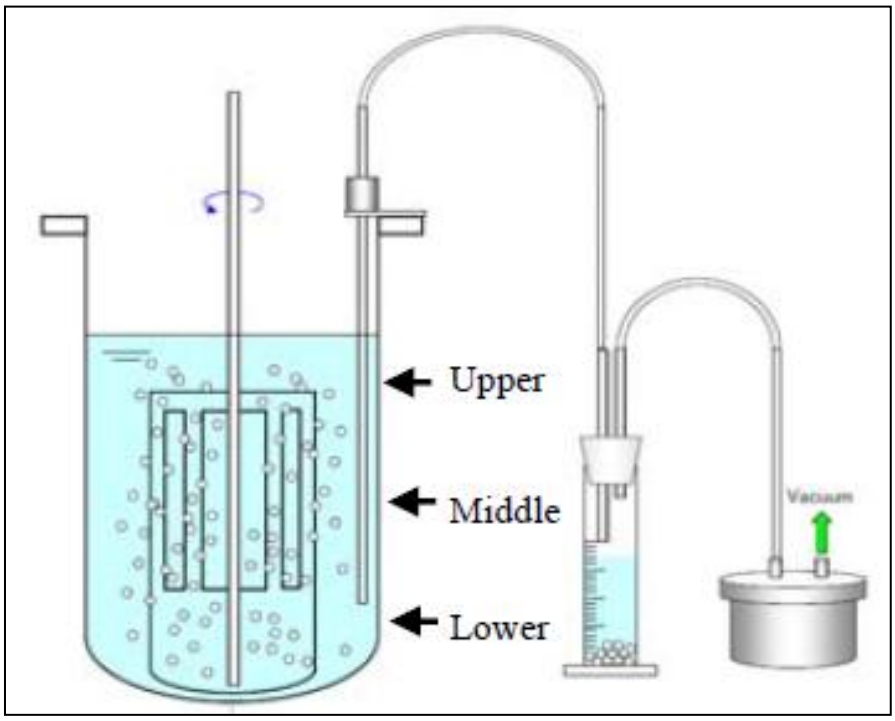

Figure 3-12: Sampling measurement system (SHI Mechanical & Equipment, 2011)

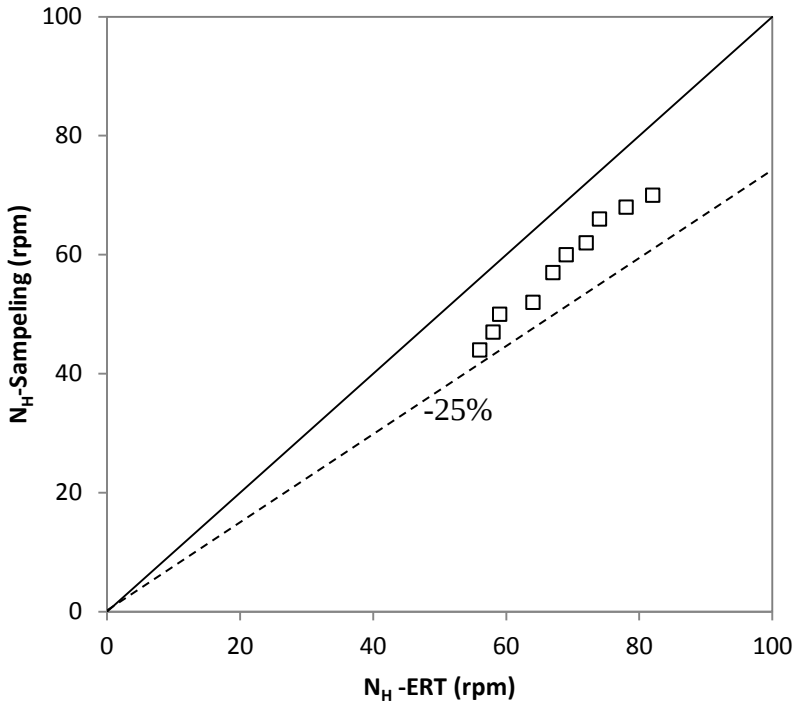

Figure 3-13: Comparison of ERT with Sampling technique (Tap water and glass beads, v=5 wt%)

3.8. Conclusions and Recommendations

The performance of Maxblend impeller for solid-liquid mixing was investigated experimentally with Newtonian fluids. Solid concentration distribution in the vessel is influenced by the operating conditions and its geometrical parameters.

Electrical resistance tomography (ERT) was successfully employed to determine the quality of solids suspension. The homogenization speed (N_H) was measured using the conductivity profile generated from the ERT data. The efficiency of Maxblend in terms of achieving uniformity was determined. The results show that particles can be homogeneously suspended with the Maxblend impeller. The particular shape of the Maxblend impeller, paddle at the bottom surmounted by a grid was demonstrated as very efficient to promote uniform suspension. The distributive motion occurring in the transient regime makes homogeneous suspension. The power consumption and dimensionless mixing time has been observed to be similar to the single phase trend.

The effect of geometry for the flat and dish bottomed vessels were investigated. The results show a 10% to 15% higher N_H in a flat bottom vessel than a dish bottom one. Because in flat-base vessels, dead zones are created between the tank base and the tank wall.

Bottom clearance has significant influence on N_H and allows for the elimination of dead zones. It was found that the minimum N_H was achieved at $C/C0$=2, lower N_H reduce the power consumption. This observation is very important for the manufacturer and could help improve the design significantly.

The concentration of solid particles also plays a crucial role in the conditions to achieve maximum homogeneity. As the concentration of solid particles increases, higher impeller speed is necessary to achieve the uniform condition. By increasing the solid concentration, the apparent viscosity and density are increased, so higher impeller speed (more power) is needed to homogenize the system.

According to the results, it can be confirmed that Maxblend is an interesting technology to obtain the uniform suspension in light of short mixing time and low power consumption.

It is useful to note some limitations of this work to inform future researchers. In this work we were limited to solids concentrations below 25 wt% (5-25 wt% solid concentration for low viscosity and 5w/w% solid concentration for high viscosity fluid) because of maximum limit of the torque measurements. The choice of the parameter to test the solids suspension capability of the Maxblend was also not trivial. While N_{js} is the main parameter to define solids suspension in literature, it was found not applicable for Maxblend impeller because of its small off-bottom clearance. A new parameter, the homogenization speed (N_H), was defined to test the performance of the Maxblend impeller for solids suspension applications. This parameter is an indicator of uniform suspension, which is different than the complete off-bottom suspension that is determined with N_{js}. This also led to the lack of comparison with literature data since there is no published data available for N_H.

With the light of these information further investigations could include the following:

- Detailed information on solid motion in agitated vessel will help to extend the current knowledge about solid suspension and dispersion mechanism with Maxblend.
- Characterizing N_H in more viscous and non-Newtonian fluids and solids dispersion and its mechanism in viscous and non-Newtonian fluids.

- Detailed information of solid concentration profile, scale effect and solid motion in Maxblend systems will extent the knowledge level to achieve a more reliable design and better operating conditions.
- This study can be extended by considering other types of Maxblend (wedge vs straight) and also with other new generation impellers like Superblend.
- Studying on a similar hydrodynamic Maxblend industrial scale (several m^3) to verify the effect of undercuts on the mixing time and segregated zones and validate tolerance established on it.

RERERENCES

ALTWAY, A., SETYWAN, H. & WINARDI, S. 2001. Effect of Particle Size on Simulation of Three-Dimensional Solid Dispersion in Stirred Tank. *Chemical Engineering Research and Design,* 79**,** 1011-1016.

ANGST, R. & KRAUME, M. 2006. Experimental investigations of stirred solid/liquid systems in three different scales: Particle distribution and power consumption. *Chemical Engineering Science,* 61**,** 2864-2870.

ARMENANTE, P. M. & NAGAMINE, E. U. 1998. Effect of low off-bottom impeller clearance on the minimum agitation speed for complete suspension of solids in stirred tanks. *Chemical Engineering Science,* 53**,** 1757-1775.

ARMENANTE, P. M., NAGAMINE, E. U. & SUSANTO, J. 1998. Determination of correlations to predict the minimum agitation speed for complete solid suspension in agitated vessels. *The Canadian Journal of Chemical Engineering,* 76**,** 413-419.

AYRANCI, I. & KRESTA, S. M. 2011. Design rules for suspending concentrated mixtures of solids in stirred tanks. *Chemical Engineering Research and Design*.

BALDI, G., CONTI, R. & ALARIA, E. 1978. Complete suspension of particles in mechanically agitated vessels. *Chemical Engineering Science,* 33**,** 21-25.

BARARPOUR, S., FRADETTE, L. & TANGUY, P. 2007. Laminar and Slurry Blending Characteristics of a Dual Shaft Impeller System. *Chemical Engineering Research and Design,* 85**,** 1305-1313.

BARRESI, A. & BALDI, G. 1987. Solid dispersion in an agitated vessel: effect of particle shape and density. *Chemical engineering science,* 42**,** 2969-2972.

BISWAS, P. K., DEV, S. C., GODIWALLA, K. M. & SIVARAMAKRISHNAN, C. S. 1999. Effect of some design parameters on the suspension characteristics of a mechanically agitated sand–water slurry system. *Materials & Design,* 20**,** 253-265.

BITTORF, K. & KRESTA, S. 2003. Prediction of Cloud Height for Solid Suspensions in Stirred Tanks. *Chemical Engineering Research and Design,* 81**,** 568-577.

BLANC, R. & GUYON, E. 1991. La Physique de la Sedimentation. *La Recherche***,** 866-873.

BOHNET, M. A. G. N. 1980. Distribution of solids in stirred suspensions. *Ger. Chem. Eng*.

BOURNE, J. & SHARMA, R. 1974a. Homogeneous particle suspension in propeller-agitated flat bottomed tanks. *The Chemical Engineering Journal,* 8**,** 243-250.

BOURNE, J. R. & SHARMA, R. N. 1974b. Homogeneous particle suspension in propeller-agitated flat bottomed tanks. *The Chemical Engineering Journal,* 8**,** 243-250.

BOYER, C., DUQUENNE, A.-M. & WILD, G. 2002. Measuring techniques in gas–liquid and gas–liquid–solid reactors. *Chemical Engineering Science,* 57**,** 3185-3215.

BUJALSKI, W., TAKENAKA, K., PAOLENI, S., JAHODA, M., PAGLIANTI, A., TAKAHASHI, K., NIENOW, A. & ETCHELLS, A. 1999. Suspension and Liquid Homogenization in High Solids Concentration Stirred Chemical Reactors. *Chemical Engineering Research and Design,* 77**,** 241-247.

BUURMAN, C., RESOORT, G. & PLASCHKES, A. 1986. Scaling-up rules for solids suspension in stirred vessels. *Chemical Engineering Science,* 41**,** 2865-2871.

CHAOUKI, J., LARACHI, F. & DUDUKOVIĆ, M. P. 1997. Noninvasive Tomographic and Velocimetric Monitoring of Multiphase Flows. *Industrial & Engineering Chemistry Research,* 36**,** 4476-4503.

CHAPMAN, C., NIENOW, A., COOKE, M. & MIDDLETON, J. 1983. Particle-Gas-Liquid Mixing in Stirred Vessels-Part II: Gas-Liquid Mixing. *Chemical engineering research and design,* 61**,** 82-95.

CHUDACEK, M. W. 1985. Solids suspension behaviour in profiled bottom and flat bottom mixing tanks. *Chemical Engineering Science,* 40**,** 385-392.

COOKE, M. & HEGGS, P. J. 2005. Advantages of the hollow (concave) turbine for multi-phase agitation under intense operating conditions. *Chemical Engineering Science,* 60**,** 5529-5543.

DEVALS, C., HENICHE, M., TAKENAKA, K. & TANGUY, P. 2008. CFD analysis of several design parameters affecting the performance of the Maxblend impeller. *Computers & Chemical Engineering,* 32**,** 1831-1841.

DOHI, N., TAKAHASHI, T., MINEKAWA, K. & KAWASE, Y. 2004. Power consumption and solid suspension performance of large-scale impellers in gas–liquid–solid three-phase stirred tank reactors. *Chemical Engineering Journal,* 97**,** 103-114.

EINENKEL, W. 1980. Influence of physical properties and equipment design on the homogeneity of suspensions in agitated vessels. *German Chemical Engineering,* 3**,** 118-124.

FAJNER, D., PINELLI, D., GHADGE, R., MONTANTE, G., PAGLIANTI, A. & MAGELLI, F. 2008. Solids distribution and rising velocity of buoyant solid particles in a vessel stirred with multiple impellers. *Chemical Engineering Science,* 63**,** 5876-5882.

FLETCHER, D. F. & BROWN, G. J. 2009. Numerical simulation of solid suspension via mechanical agitation: effect of the modelling approach, turbulence model and hindered settling drag law. *International Journal of Computational Fluid Dynamics,* 23**,** 173-187.

FOUCAULT, S., ASCANIO, G. & TANGUY, P. A. 2004. Coaxial Mixer Hydrodynamics with Newtonian and non-Newtonian Fluids. *Chemical Engineering & Technology,* 27**,** 324-329.

FRADETTE, L., TANGUY, P. A., BERTRAND, F., THIBAULT, F., RITZ, J.-B. & GIRAUD, E. 2007a. CFD phenomenological model of solid–liquid mixing in stirred vessels. *Computers & Chemical Engineering,* 31**,** 334-345.

FRADETTE, L., THOME, G., TANGUY, P. & TAKENAKA, K. 2007b. Power and Mixing Time Study Involving a Maxblend® Impeller with Viscous Newtonian and Non-Newtonian Fluids. *Chemical Engineering Research and Design,* 85**,** 1514-1523.

FUENTE, E. B.-D. L. A., CHOPLIN, L. & TANGUY, P. A. 1997. Mixing With Helical Ribbon Impellers : Effect of Highly Shear Thinning Behaviour and Impeller Geometry.

GHIONZOLI, A., BUJALSKI, W., GRENVILLE, R., NIENOW, A., SHARPE, R. & PAGLIANTI, A. 2007. The Effect of Bottom Roughness on the Minimum Agitator Speed Required to Just Fully Suspend Particles in a Stirred Vessel. *Chemical Engineering Research and Design,* 85**,** 685-690.

GIGUÈRE, R., FRADETTE, L., MIGNON, D. & TANGUY, P. 2008. Characterization of slurry flow regime transitions by ERT. *Chemical Engineering Research and Design,* 86**,** 989-996.

GILLIES, R. G., HILL, K. B., MCKIBBEN, M. J. & SHOOK, C. A. 1999. Solids transport by laminar Newtonian flows. *Powder Technology,* 104**,** 269-277.

GODFREY, J. & ZHU, Z. 1994. Measurement of particle-liquid profiles in agitated tanks. *AIChE Symposium Series.* New York, NY: American Institute of Chemical Engineers, 1971-c2002.

GUIRAUD, P., COSTES, J. & BERTRAND, J. 1997. Local measurements of fluid and particle velocities in a stirred suspension. *Chemical Engineering Journal,* 68**,** 75-86.

GUNTZBURGER, Y., FRADETTE, L., FARHAT, M., HÉNICHE, M., TANGUY, P. A. & TAKENAKA, K. 2009. Effect of the geometry on the performance of the Maxblend™ impeller with viscous Newtonian fluids. *Asia-Pacific Journal of Chemical Engineering,* 4**,** 528-536.

HARNBY, N., EDWARDS, M. F. & NIENOW, A. W. 1997. Mixing in the process industries. 432.

HICKS, M. T., MYERS, K. J. & BAKKER, A. 1997. Cloud Height in Solids Suspension Agitation. *Chemical Engineering Communications,* 160**,** 137-155.

HOLLAND, F. & CHAPMAN, F. 1966. Liquid mixing and processing in stirred tanks.

HOSSEINI, S., PATEL, D., EIN-MOZAFFARI, F. & MEHRVAR, M. 2010a. Study of Solid-Liquid Mixing in Agitated Tanks through Computational Fluid Dynamics Modeling. *Society***,** 4426-4435.

HOSSEINI, S., PATEL, D., EIN-MOZAFFARI, F. & MEHRVAR, M. 2010b. Study of solid–liquid mixing in agitated tanks through electrical resistance tomography. *Chemical Engineering Science,* 65**,** 1374-1384.

IBRAHIM, S. B. & NIENOW, A. W. 1994. The effect of viscosity on mixing pattern and solid suspension in stirred vessels. *Institution os chemical engineers symposium series.* Hemsphere publishing corporation.

IRANSHAHI, A., DEVALS, C., HENICHE, M., FRADETTE, L., TANGUY, P. A. & TAKENAKA, K. 2007. Hydrodynamics characterization of the Maxblend impeller. *Chemical Engineering Science,* 62**,** 3641-3653.

JAFARI, R. 2010. *Solid Suspension and Gas Dispersion in Mechanically Agitated Vessels.* École Polytechnique de Montréal.

JINESCU, V. 1974. The rheology of suspensions. *Int. Chem. Eng,* 14**,** 397-420.

KEE, N. & TAN, R. B. H. 2002. CFD simulation of solids suspension in mixing vessels. *The Canadian Journal of Chemical Engineering,* 80**,** 1-6.

KIM, S., NKAYA, A. & DYAKOWSKI, T. 2006. Measurement of mixing of two miscible liquids in a stirred vessel with electrical resistance tomography☆. *International Communications in Heat and Mass Transfer,* 33**,** 1088-1095.

KRESTA, S. M. & WOOD, P. E. 1993. The mean flow field produced by a 45 pitched blade turbine: changes in the circulation pattern due to off bottom clearance. *The Canadian Journal of Chemical Engineering,* 71**,** 42-53.

KURATSU, M., YATOMI, R. & SAITOH, H. 1995. Design of versatile reactors. *Chemical Equipment,* 8**,** 86-92.

LEA, J. 2009. Suspension Mixing Tank-Design Heuristic. *Chemical Product and Process Modeling,* 4**,** 17.

LEHN, M. C., MYERS, K. J. & BARKER, A. 1999. Agitator design for solids suspension under gassed conditions. *The Canadian Journal of Chemical Engineering,* 77**,** 1065-1071.

MACTAGGART, R. S., NASR-EL-DIN, H. A. & MASLIYAH, J. H. 1993. Sample withdrawal from a slurry mixing tank. *Chemical Engineering Science,* 48**,** 921-931.

MAGELLI, F., FAJNER, D., NOCENTINI, M., PASQUALI, G., MARISKO, V. & DITL, P. 1991. Solids concentration distribution in slurry reactors stirred with multiple axial impellers. *Chemical Engineering and Processing: Process Intensification,* 29**,** 27-32.

MAUDE, A. D. & WHITMORE, R. L. 1958. A generalized theory of sedimentation. *British Journal of Applied Physics,* 9**,** 477-482.

MCDONOUGH, R. 1992. Mixing for the process industries.

MCMILLAN, G. K., CONSIDINE, D. M. & EBRARY, I. 1999. Process/industrial instruments and controls handbook.

METZNER, A. B. & OTTO, R. E. 1957. Agitation of non-Newtonian fluids. *AIChE Journal,* 3**,** 3-10.

MICALE, G., GRISAFI, F. & BRUCATO, A. 2002. Assessment of Particle Suspension Conditions in Stirred Vessels by Means of Pressure Gauge Technique. *Chemical Engineering Research and Design,* 80**,** 893-902.

MICALE, G., GRISAFI, F., RIZZUTI, L. & BRUCATO, A. 2004. CFD Simulation of Particle Suspension Height in Stirred Vessels. *Chemical Engineering Research and Design,* 82**,** 1204-1213.

MICALE, G., MONTANTE, G., GRISAFI, F., BRUCATO, A. & GODFREY, J. 2000. CFD Simulation of Particle Distribution in Stirred Vessels. *Chemical Engineering Research and Design,* 78**,** 435-444.

MICHELETTI, M., NIKIFORAKI, L., LEE, K. C. & YIANNESKIS, M. 2003. Particle concentration and mixing characteristics of moderate-to-dense solid-liquid suspensions. *Industrial & engineering chemistry research,* 42**,** 6236-6249.

MISHIMA, M. 1992. New trend of mixing vessel. *Chem. Eng. Japan*.

MONTANTE, G., BRUCATO, A., LEE, K. & YIANNESKIS, M. 1999. An experimental study of double-to-single-loop transition in stirred vessels. *The Canadian Journal of Chemical Engineering,* 77**,** 649-659.

MONTANTE, G., LEE, K. C., BRUCATO, A. & YIANNESKIS, M. 2001. Numerical simulations of the dependency of flow pattern on impeller clearance in stirred vessels. *Chemical Engineering Science,* 56**,** 3751-3770.

MONTANTE, G., PINELLI, D. & MAGELLI, F. 2002. Diagnosis of solid distribution in vessels stirred with multiple PBTs and comparison of two modelling approaches. *The Canadian Journal of Chemical Engineering,* 80**,** 1-9.

MURTHY, B., GHADGE, R. & JOSHI, J. 2007. CFD simulations of gas–liquid–solid stirred reactor: Prediction of critical impeller speed for solid suspension. *Chemical Engineering Science,* 62**,** 7184-7195.

MUSIL, L. & VLK, J. 1978. Suspending solid particles in an agitated conical-bottom tank. *Chemical Engineering Science,* 33**,** 1123-1131.

NASR-EL-DIN, H. A., MAC TAGGART, R. S. & MASLIYAH, J. H. 1996. Local solids concentration measurement in a slurry mixing tank. *Chemical Engineering Science,* 51**,** 1209-1220.

NIENOW, HARNBY & EDITORS, M. F. E. 1997. Mixing in the Process Industries : Second Edition.

OCHIENG, A. & LEWIS, A. 2006a. CFD simulation of solids off-bottom suspension and cloud height. *Hydrometallurgy,* 82**,** 1-12.

OCHIENG, A. & LEWIS, A. E. 2006b. Nickel solids concentration distribution in a stirred tank. *Minerals Engineering,* 19**,** 180-189.

OSHINOWO, L. M. B., ANDRE. 2002. CFD MODELING OF SOLIDS SUSPENSIONS IN STIRRED TANKS.

PANNEERSELVAM, R., SAVITHRI, S. & SURENDER, G. D. 2008. Computational Fluid Dynamics Simulation of Solid Suspension in a Gas- Liquid- Solid Mechanically Agitated Contactor. *Industrial & Engineering Chemistry Research,* 48**,** 1608-1620.

PASQUALI, G., FAJNER, D. & MAGELLI, F. 1983. EFFECT OF SUSPENSION VISCOSITY ON POWER CONSUMPTION IN THE AGITATION OF SOLID-LIQUID SYSTEMS. *Chemical Engineering Communications,* 22**,** 371-375.

PAUL, E. L., ATIEMO-OBENG, V. A. & KRESTA, S. M. 2004. Handbook of industrial mixing.

PEKER, S. M. & HELVACı, Ş. Ş. 2007. Solid-liquid two phase flow (Google eBook). 2007**,** 515.

PINELLI, D. & MAGELLI, F. 2001. Solids settling velocity and distribution in slurry reactors with dilute pseudoplastic suspensions. *Industrial & engineering chemistry research,* 40**,** 4456-4462.

REWATKAR, V. B., RAO, K. S. M. S. R. & JOSHI, J. B. 1991. Critical impeller speed for solid suspension in mechanically agitated three-phase reactors. 1. Experimental part. *Industrial & Engineering Chemistry Research,* 30**,** 1770-1784.

SARDESHPANDE, M. V., SAGI, A. R., JUVEKAR, V. A. & RANADE, V. V. 2009. Solid Suspension and Liquid Phase Mixing in Solid−Liquid Stirred Tanks. *Industrial & Engineering Chemistry Research,* 48**,** 9713-9722.

SHAMLOU, P. A. 1993. Processing of solid-liquid suspensions.

SHAMLOU, P. A. & KOUTSAKOS, E. 1989. Solids suspension and distribution in liquids under turbulent agitation. *Chemical Engineering Science,* 44**,** 529-542.

SHARMA, R. & SHAIKH, A. 2003. Solids suspension in stirred tanks with pitched blade turbines. *Chemical Engineering Science,* 58**,** 2123-2140.

SOLOMON, J., ELSON, T. P., NIENOW, A. W. & PACE, G. W. 1981. Cavern sizes in agitated fluids with a yield stress. *Chemical Engineering Communications,* 11**,** 143-164.

SPIDLA, M. & SINEVIC, V. 2005. Solid particle distribution of moderately concentrated suspensions in a pilot plant stirred vessel. *Chemical Engineering …*.

SUMI, Y. & KAMIWANO, M. 2001. Development and mixing characteristics of a multistage impeller for agitating highly viscous fluids. *Journal of chemical engineering of Japan*.

TAHVILDARIAN, P., NG, H., D'AMATO, M., DRAPPEL, S., EIN-MOZAFFARI, F. & UPRETI, S. R. 2011. Using electrical resistance tomography images to characterize the mixing of micron-sized polymeric particles in a slurry reactor. *Chemical Engineering Journal*.

TAKAHASHI, T., TAGAWA, A., ATSUMI, N., DOHI, N. & KAWASE, Y. 2006. Liquid-phase mixing time in boiling stirred tank reactors with large cross-section impellers. *Chemical Engineering and Processing: Process Intensification,* 45**,** 303-311.

TAMBURINI, A., CIPOLLINA, A., MICALE, G., CIOFALO, M. & BRUCATO, A. 2009. Dense Solid-Liquid Off-Bottom Suspension Dynamics : Simulation and Experiment. *Simulation***,** 14-17.

TANGUY, P. A., THIBAULT, F., BRITO-DE LA FUENTE, E., ESPINOSA-SOLARES, T. & TECANTE, A. 1997. Mixing performance induced by coaxial flat blade-helical ribbon impellers rotating at different speeds. *Chemical Engineering Science,* 52**,** 1733-1741.

UHL, V. W. & GRAY, J. B. 1986. Mixing: theory and practice. Volume III.

WILLIAMS, R. A. & BECK, M. S. 1995. Process tomography: principles, techniques, and applications.

WU, J., ZHU, Y. & PULLUM, L. 2001. Impeller geometry effect on velocity and solids suspension. *Chemical Engineering Research and Design,* 79**,** 989-997.

WU, J., ZHU, Y. G. & PULLUM, L. 2002. Suspension of high concentration slurry. *AIChE Journal,* 48**,** 1349-1352.

XU, Y., DONG, F. & TAN, C. 2010. Electrical resistance tomography for locating inclusions using analytical boundary element integrals and their partial derivatives. *Engineering Analysis with Boundary Elements,* 34**,** 876-883.

YAMAMURA, K. & HIRUTA, O. 1997. Application of Maxblend Fermentor @ for Microbial Processes. *Journal of Fermentation and Bioengineering,* 83**,** 79-86.

YAMAZAKI, H., TOJO, K. & MIYANAMI, K. 1986. Concentration profiles of solids suspended in a stirred tank. *Powder Technology,* 48**,** 205-216.

YAO, W., MISHIMA, M. & TAKAHASHI, K. 2001. Numerical investigation on dispersive mixing characteristics of MAXBLEND and double helical ribbons. *Chemical Engineering Journal,* 84**,** 565-571.

ZLOKARNIK, M. 2001. Stirring: theory and practice. 362.

ZWIETERING, T. N. 1958. Suspending of solid particles in liquid by agitators. *Chemical Engineering Science,* 8**,** 244-253.